Multiple timescale simulations of global macroscopic dynamics of magnetized plasma

Stephen C. Jardin[1]
N.M. Ferraro[2], **J. Breslau**[1], **J. Chen**[1],

[1]*Princeton Plasma Physics Laboratory*
[2] *General Atomics*

IPAM Workshop
Computational Challenges in Magnetized Plasma

University of California, Los Angeles
April 17, 2012

This work was performed in close collaboration with M. Shephard, F. Zhang, and F. Delalondre at the SCOREC center at Rensselaer Polytechnic Institute in Troy, NY.

Acknowledgements also to: G. Fu, S. Hudson, H. Strauss, L. Sugiyama

For magnetic confinement, there are 4 classes of major simulation codes, each addressing different phenomena

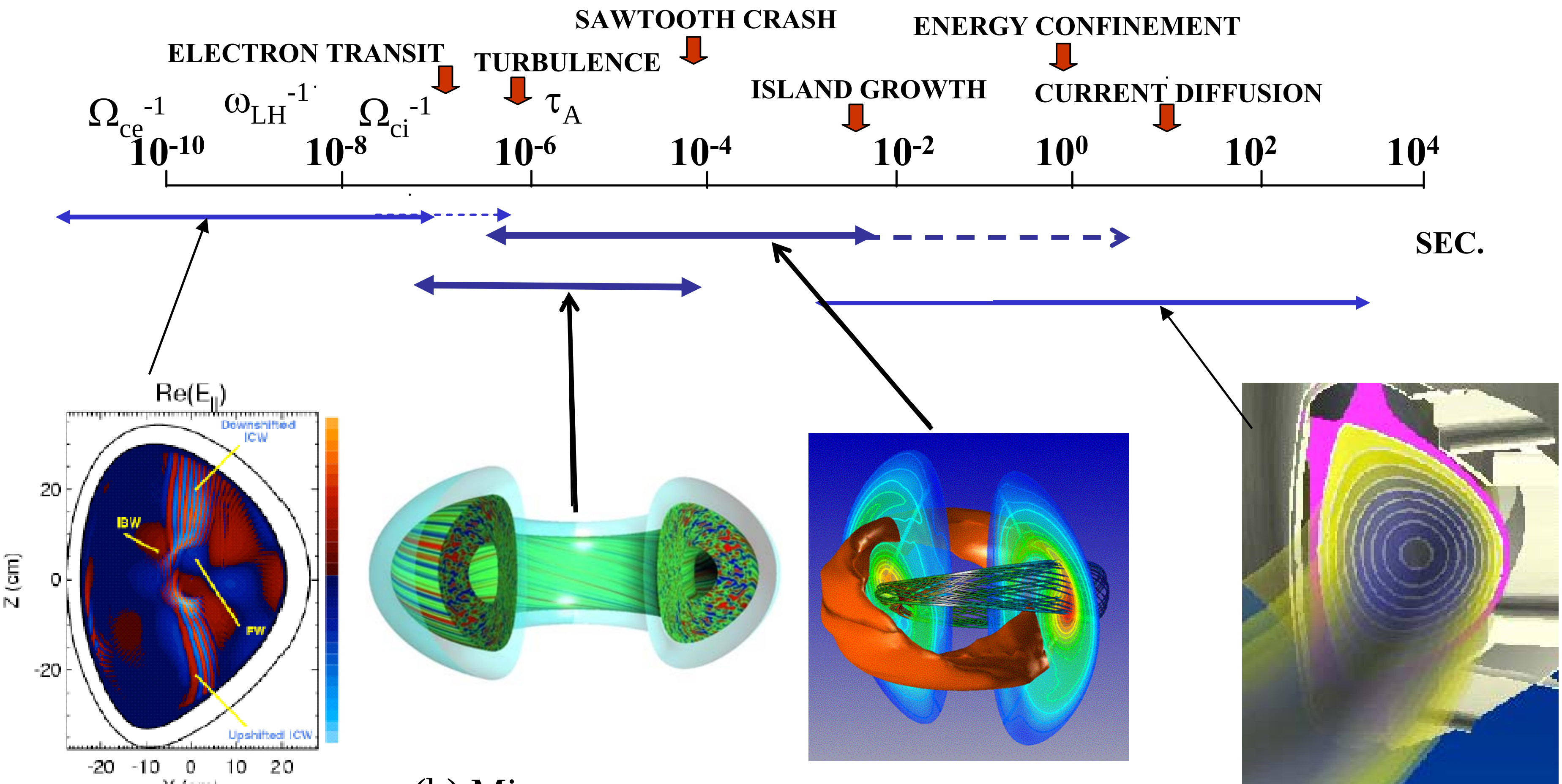

(a) RF codes

(b) Micro-turbulence codes

(c) Extended-MHD codes

(d) Transport Codes

Summary and Overview:

- 3D MHD equations are a mixed system: hyperbolic + parabolic
  - This leads to multiple timescales in a magnetized plasma

- The hyperbolic terms are associated with *ideal MHD* wave propagation and global instabilities.
  - These are the shortest timescales: typically micro-seconds

- The parabolic terms are associated with *diffusion and transport* of the magnetic field, current, pressures, and densities
  - These are the longest timescales: typically 100s of milliseconds

- To calculate both phenomena in a single simulation requires a highly *implicit* formulation so that the time step is determined by accuracy requirements only
  - not by numerical stability requirements such as Courant condition

- The implicit solution procedure is complicated by the fact that the multiple timescales present in the physics lead to a very *ill-conditioned* matrix equation that needs to be solved each time step.
  - Here we describe the techniques we use to deal with this in M3D-C^1

2-Fluid 3D MHD Equations:

$$\frac{\partial n}{\partial t} + \nabla \bullet (n\mathbf{V}) = 0$$ continuity

$$\frac{\partial \mathbf{B}}{\partial t} = -\nabla \times \mathbf{E} \qquad \nabla \bullet \mathbf{B} = 0 \qquad \mu_0 \mathbf{J} = \nabla \times \mathbf{B}$$ Maxwell

$$nM_i\left(\frac{\partial \mathbf{V}}{\partial t} + \mathbf{V} \bullet \nabla \mathbf{V}\right) + \nabla p = \mathbf{J} \times \mathbf{B} - \nabla \bullet \mathbf{\Pi}_{GV} - \nabla \bullet \mathbf{\Pi}_{\mu}$$ momentum

$$\mathbf{E} + \mathbf{V} \times \mathbf{B} = \eta \mathbf{J} + \frac{1}{ne}\left(\mathbf{J} \times \mathbf{B} - \nabla p_e - \nabla \bullet \mathbf{\Pi}_e\right)$$ Ohm's law

$$\frac{3}{2}\frac{\partial p_e}{\partial t} + \nabla \bullet \left(\frac{3}{2} p_e \mathbf{V}\right) = -p_e \nabla \bullet \mathbf{V} + \eta J^2 - \nabla \bullet \mathbf{q}_e + Q_\Delta$$ electron energy

$$\frac{3}{2}\frac{\partial p_i}{\partial t} + \nabla \bullet \left(\frac{3}{2} p_i \mathbf{V}\right) = -p_i \nabla \bullet \mathbf{V} - \mathbf{\Pi}_\mu \bullet \nabla \mathbf{V} - \nabla \bullet \mathbf{q}_i - Q_\Delta$$ ion energy

Ideal MHD

Resistive MHD

2-fluid MHD

The objective of the **M3D-*C*[1]** project is to solve these equations as accurately as possible in 3D toroidal geometry with realistic B.C. and optimized for a low-β torus with a strong toroidal field.

Contain ideal MHD, reconnection, and transport timescales

$$\tau_I \ll \tau_R \ll \tau_T$$

Three types of wave solutions in ideal MHD

Slow Wave

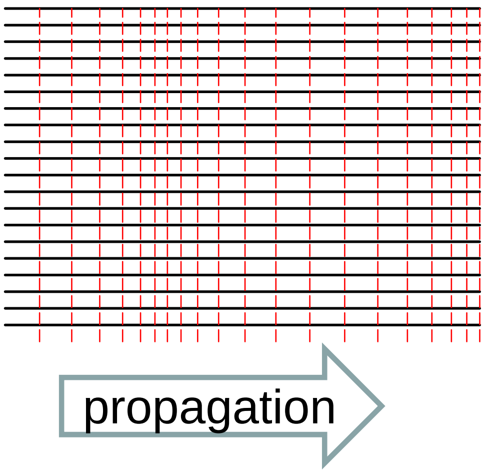

- only propagates parallel to **B**
- only compresses fluid in parallel direction
- does not perturb magnetic field

Alfven Wave

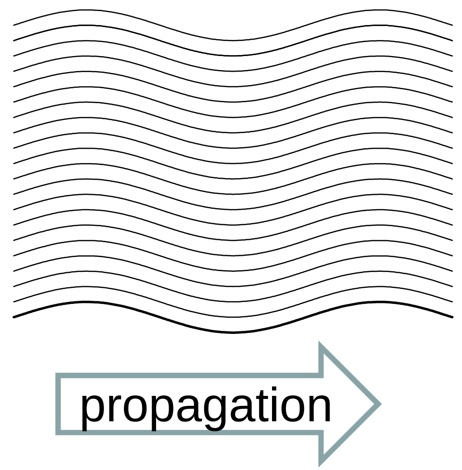

- only propagates parallel to **B**
- incompressible
- only bends the field, does not compress it

Fast Wave

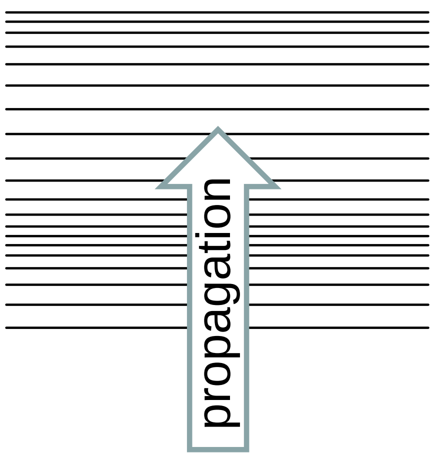

- can propagate perpendicular to **B**
- only compresses fluid in $\perp$ direction
- compresses the magnetic field

Three types of wave solutions in ideal MHD

Slow Wave

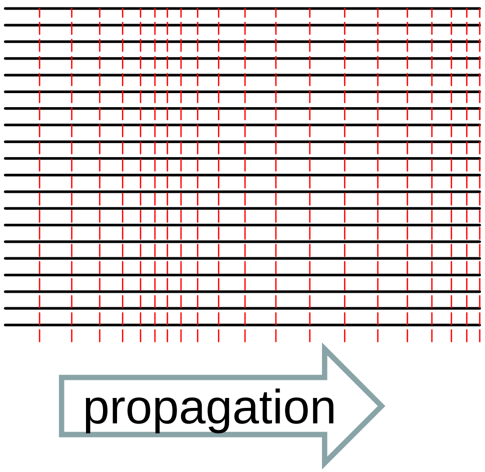

- only propagates parallel to **B**
- only compresses fluid in parallel direction
- does not perturb magnetic field

Alfven Wave

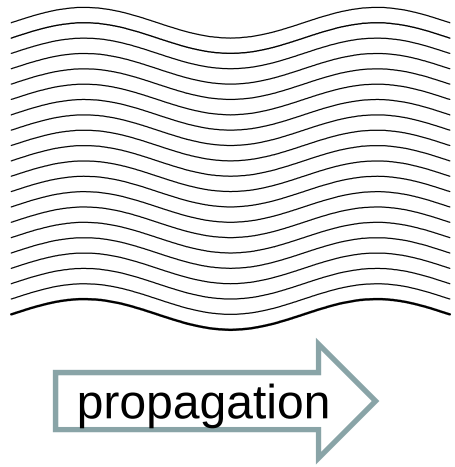

- only propagates parallel to **B**
- incompressible
- only bends the field, does not compress it

Plasma instabilities grow out of these two waves

Fast Wave

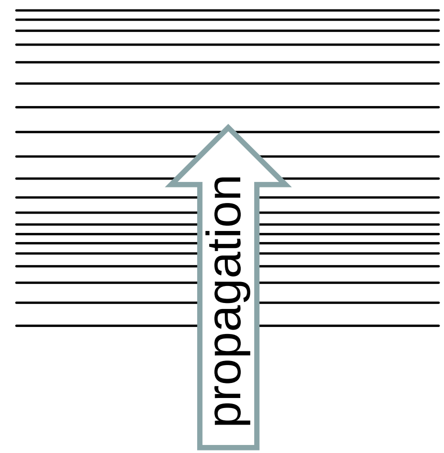

- can propagate perpendicular to **B**
- only compresses fluid in $\perp$ direction
- compresses the magnetic field

•This is the wave that makes equations stiff!

The three ideal MHD waves have widely separate velocities for propagation with $\mathbf{k} \bullet \mathbf{B} \sim 0$

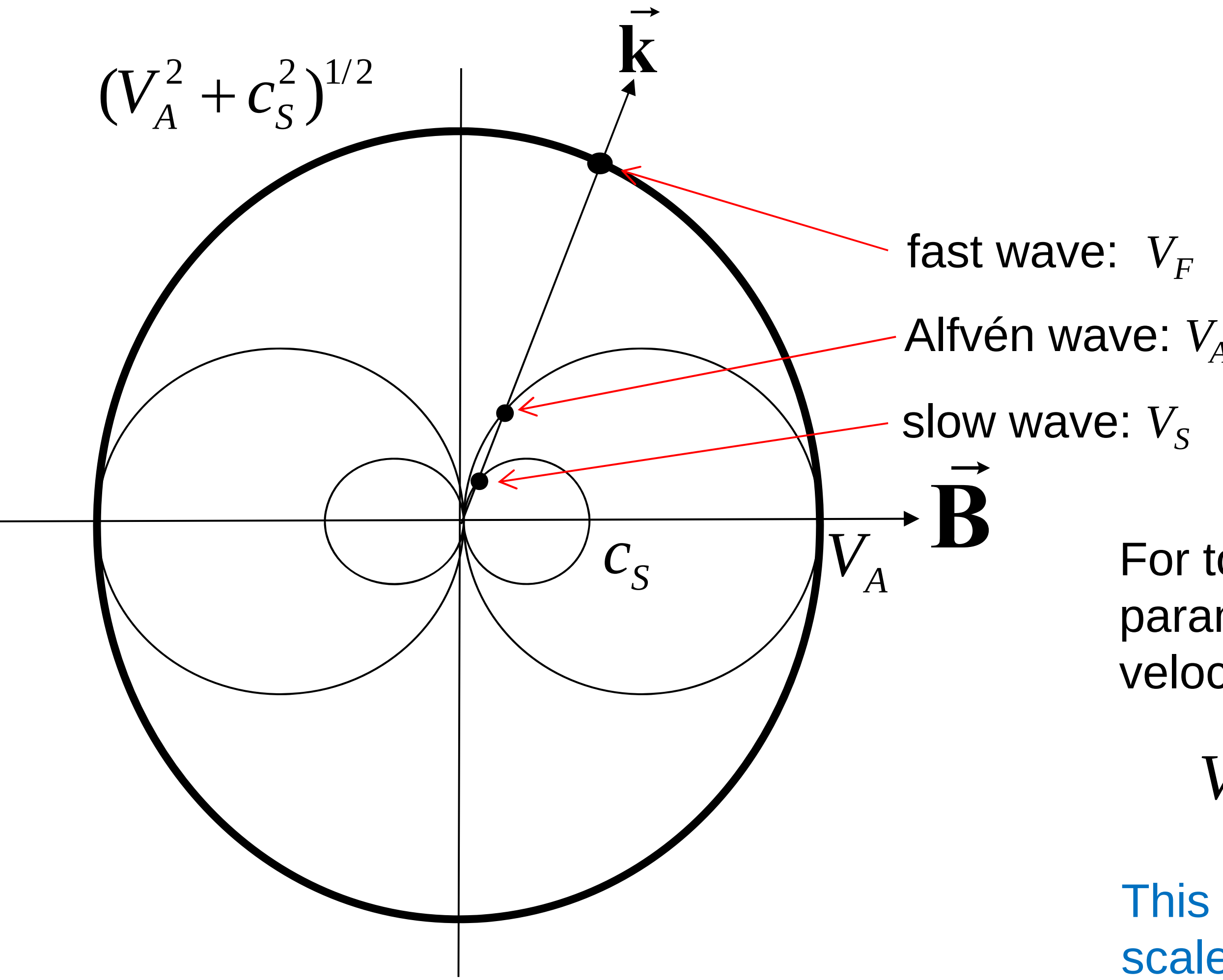

Wave speed diagram for ideal MHD. Intersection points show wave velocity for given propagation direction.

For tokamak geometry and parameters, the three wave velocities satisfy the inequalities:

$$V_F \gg V_A \gg V_S$$

This leads to multiple time-scales, even within ideal MHD

Implicit solution requires evaluating the spatial derivatives at the new time level.

The advantage of an implicit solution is that the time step can be very large and still be numerically stable (no Courant condition)

If we discretize in space (finite difference, finite element, or spectral) and linearize the equations about the present time level, the implicit equations take the form:

$$\begin{bmatrix} \mathbf{A}_{11} & \mathbf{A}_{12} & \mathbf{A}_{13} \\ \mathbf{A}_{21} & \mathbf{A}_{22} & \mathbf{A}_{23} \\ \mathbf{A}_{31} & \mathbf{A}_{32} & \mathbf{A}_{33} \end{bmatrix} \bullet \begin{bmatrix} \mathbf{V} \\ \mathbf{B} \\ p \end{bmatrix}^{n+1} = \begin{bmatrix} \mathbf{r}_1 \\ \mathbf{r}_2 \\ \mathbf{r}_3 \end{bmatrix}^{n}$$

Very large, ~ (10^7 x 10^7)
non-diagonally dominant,
non-symmetric, ill-conditioned sparse matrix (contains all MHD waves)

Implicit solution requires evaluating the spatial derivatives at the new time level.

The advantage of an implicit solution is that the time step can be very large and still be numerically stable (no Courant condition)

If we discretize in space (finite difference, finite element, or spectral) and linearize the equations about the present time level, the implicit equations take the form:

$$\begin{bmatrix} \mathbf{A}_{11} & \mathbf{A}_{12} & \mathbf{A}_{13} \\ \mathbf{A}_{21} & \mathbf{A}_{22} & \mathbf{A}_{23} \\ \mathbf{A}_{31} & \mathbf{A}_{32} & \mathbf{A}_{33} \end{bmatrix} \bullet \begin{bmatrix} \mathbf{V} \\ \mathbf{B} \\ p \end{bmatrix}^{n+1} = \begin{bmatrix} \mathbf{r}_1 \\ \mathbf{r}_2 \\ \mathbf{r}_3 \end{bmatrix}^{n}$$

How best to solve this?

Very large, ~ (10^7 x 10^7)
non-diagonally dominant,
non-symmetric, ill-conditioned sparse matrix (contains all MHD waves)

Preconditioned iterative method

Preconditioning

…*preconditioning* is a procedure of an application of a transformation, called the *preconditioner*, that conditions a given problem into a form that is more suitable for numerical solution. …..*Wikipedia*

$$\mathbf{A} \bullet \mathbf{X} = \mathbf{b}$$

Left preconditioning multiplies by a matrix from the left:

$$\mathbf{P} \bullet \mathbf{A} \bullet \mathbf{X} = \mathbf{P} \bullet \mathbf{b}$$

Right preconditioning multiplies by a matrix from the right:

$$\mathbf{A} \bullet \mathbf{P} \bullet \mathbf{Y} = \mathbf{b}$$

$$\mathbf{Y} = \mathbf{P}^{-1} \bullet \mathbf{X} \qquad (\text{or } \mathbf{X} = \mathbf{P} \bullet \mathbf{Y})$$

The preconditioner $\mathbf{P}$ is chosen so that $\mathbf{P\,A}$ or $\mathbf{A\,P}$ has *better properties* than the original matrix A. Most of the differences between the different 3D MHD codes is due to a difference in the preconditioning techniques.

Preconditioning

…*preconditioning* is a procedure of an application of a transformation, called the *preconditioner*, that conditions a given problem into a form that is more suitable for numerical solution. …..*Wikipedia*

$$\mathbf{A} \bullet \mathbf{X} = \mathbf{b}$$

Left preconditioning multiplies by a matrix from the left:

$$\mathbf{P} \bullet \mathbf{A} \bullet \mathbf{X} = \mathbf{P} \bullet \mathbf{b}$$

Right preconditioning multiplies by a matrix from the right:

$$\mathbf{A} \bullet \mathbf{P} \bullet \mathbf{Y} = \mathbf{b}$$

$$\mathbf{Y} = \mathbf{P}^{-1} \bullet \mathbf{X} \qquad (\text{or } \mathbf{X} = \mathbf{P} \bullet \mathbf{Y})$$

The preconditioner $\mathbf{P}$ is chosen so that $\mathbf{P}\,\mathbf{A}$ or $\mathbf{A}\,\mathbf{P}$ has *better properties* than the original matrix A. Most of the differences between the different 3D MHD codes is due to a difference in the preconditioning techniques.

Here we use a 3-level preconditioner that is motivated by the physics of MHD phenomena in tokamaks.

More on Preconditioning

From:

L. N. Trefethen and D. Bau, III, Numerical Linear Algebra (SIAM) 1997

“In ending this book with the subject of preconditioners, we find ourselves at the philosophical center of the scientific computing of the future…

Nothing will be more central to computational science in the next century than the art of transforming a problem that appears intractable into another whose solution can be approximated rapidly.

For Krylov subspace matrix iterations, this is *preconditioning*.”

Still more on Preconditioning

“ Direct solvers are often the best option for 2-dimensional problems, but not for 3-dimensional problems.

Generally speaking, preconditioning attempts to *improve the spectral properties of the coefficient matrix.* For symmetric positive definite problems, the rate of convergence of the CG method depends on the spectral radius.

For non-symmetric problems, the situation is more complicated and the eigenvalues may not describe the convergence properties. Nevertheless, *a clustered spectrum (away from 0) often results in rapid convergence, particularly when the preconditioned matrix is close to normal. “*

FROM: *Michele Benzi, “Preconditioning Techniques for Large Linear Systems: A Survey”, J. Comput. Phys. 182, 418-477 (2002)*

Still more on Preconditioning

" Direct solvers are often the best option for 2-dimensional problems, but not for 3-dimensional problems.

Generally speaking, preconditioning attempts to *improve the spectral properties of the coefficient matrix.* For symmetric positive definite problems, the rate of convergence of the CG method depends on the spectral radius.

For *non-symmetric problems*, the situation is more complicated and the eigenvalues may not describe the convergence properties. Nevertheless, *a clustered spectrum (away from 0) often results in rapid convergence, particularly when the preconditioned matrix is close to normal.* "

Make the matrix (close to) symmetric + Reduce the spectral radius (using 2D direct solves if needed)

$$\rho(A) \equiv \frac{|\lambda|_{\max}}{|\lambda|_{\min}}$$

FROM: *Michele Benzi, "Preconditioning Techniques for Large Linear Systems: A Survey", J. Comput. Phys. 182, 418-477 (2002)*

3 step physics-based preconditioner greatly improves iterative solve

(1) Split implicit formulation

(2) Apply annihilation operators

(3) Apply block-Jacobi preconditioner by using SuperLU_dist on each poloidal plane independently

Original matrix multiplying
V^{n+1}, **B**$^{n+1}$, p^{n+1}
- non-symmetric,
- non-diagonally dominant &
- large range of eigenvalues

→ [ ] → [[ ] [ ] [ ]] → [[ ] [ ] [ ]] → GMRES

Smaller matrix multiplying **V**$^{n+1}$ only,
- nearly symmetric
- closer to diagonal
- still with large range of eigenvalues

Matrix now consists of 3 dominant diagonal blocks, each with narrower range of eigenvalues.

Now, range of eigenvalues in each block is greatly reduced.

Preconditioned system converges in 10's of iterations

3 step physics-based preconditioner greatly improves iterative solve

(1) Split implicit formulation

(2) Apply annihilation operators

(3) Apply block-Jacobi preconditioner by using SuperLU_dist on each poloidal plane independently

Original matrix multiplying
V^{n+1}, **B**$^{n+1}$, p^{n+1}
- non-symmetric,
- non-diagonally dominant &
- large range of eigenvalues

→ [ ] → [[ ] [ ] [ ]] → [[ ] [ ] [ ]] → GMRES

Smaller matrix multiplying **V**$^{n+1}$ only,
- nearly symmetric
- closer to diagonal
- still with large range of eigenvalues

Matrix now consists of 3 dominant diagonal blocks, each with narrower range of eigenvalues.

Now, range of eigenvalues in each block is greatly reduced.

Preconditioned system converges in 10's of iterations

(1) Split implicit formulation eliminates $\mathbf{B}^{n+1}$ and p^{n+1} in favor of $\mathbf{V}^{n+1}$

As an example, consider the simple 1D wave equation for velocity V and pressure p

$$\left.\begin{aligned}\frac{\partial V}{\partial t} &= c\frac{\partial p}{\partial x}\\ \frac{\partial p}{\partial t} &= c\frac{\partial V}{\partial x}\end{aligned}\right\} \quad \frac{\partial^2 V}{\partial t^2} - c^2\frac{\partial^2 V}{\partial x^2} = 0$$

Implicit FD time advance evaluates spatial derivatives at the new time level

$$\frac{V_j^{n+1} - V_j^n}{\delta t} = c\left(\frac{p_{j+1/2}^{n+1} - p_{j-1/2}^{n+1}}{\delta x}\right)$$

$$\frac{p_{j+1/2}^{n+1} - p_{j+1/2}^{n}}{\delta t} = c\left(\frac{V_{j+1}^{n+1} - V_j^{n+1}}{\delta x}\right)$$

(1) Split implicit formulation eliminates $\mathbf{B}^{n+1}$ and p^{n+1} in favor of $\mathbf{V}^{n+1}$

As an example, consider the simple 1D wave equation for velocity V and pressure p

$$\left.\begin{aligned} \frac{\partial V}{\partial t} &= c\frac{\partial p}{\partial x} \\ \frac{\partial p}{\partial t} &= c\frac{\partial V}{\partial x} \end{aligned}\right\} \quad \frac{\partial^2 V}{\partial t^2} - c^2\frac{\partial^2 V}{\partial x^2} = 0$$

Implicit FD time advance evaluates spatial derivatives at the new time level

$$\frac{V_j^{n+1} - V_j^n}{\delta t} = c\left(\frac{\boxed{p_{j+1/2}^{n+1}} - p_{j-1/2}^{n+1}}{\delta x}\right)$$

$$\frac{\boxed{p_{j+1/2}^{n+1}} - p_{j+1/2}^{n}}{\delta t} = c\left(\frac{V_{j+1}^{n+1} - V_j^{n+1}}{\delta x}\right)$$

Now, algebraically eliminate new time pressure in favor of velocity

$$V_j^{n+1} = V_j^n + (\delta t c)^2\left(\frac{V_{j+1}^{n+1} - 2V_j^{n+1} + V_{j-1}^{n+1}}{\delta x^2}\right) + \delta t c\left(\frac{p_{j+1/2}^{n} - p_{j-1/2}^{n}}{\delta x}\right) \quad \leftarrow$$

Symmetric & diagonally dominant!

$$p_{j+1/2}^{n+1} = p_{j+1/2}^{n} + \frac{\delta t c}{\delta x}\left(V_{j+1}^{n+1} - V_j^{n+1}\right)$$

These equations will give exactly the same answers, but can be solved sequentially!

Schematic of difference in matrices to be inverted after applying split implicit formulation

$$
2N \quad
\begin{bmatrix}
1 & -S & & & & & & & & & & \\
S & 1 & -S & & & & & & & & & \\
 & S & 1 & -S & & & & & & & & \\
 & & S & 1 & -S & & & & & & & \\
 & & & S & 1 & -S & & & & & & \\
 & & & & S & 1 & -S & & & & & \\
 & & & & & S & 1 & -S & & & & \\
 & & & & & & S & 1 & -S & & & \\
 & & & & & & & S & 1 & -S & & \\
 & & & & & & & & S & 1 & -S & \\
 & & & & & & & & & S & 1 & -S \\
 & & & & & & & & & & S & 1
\end{bmatrix}
$$

Coupled system multiplying V^{n+1} & p^{n+1}

$$
N \quad
\begin{bmatrix}
1+2S^2 & -S^2 & & & & \\
-S^2 & 1+2S^2 & -S^2 & & & \\
 & -S^2 & 1+2S^2 & -S^2 & & \\
 & & -S^2 & 1+2S^2 & -S^2 & \\
 & & & -S^2 & 1+2S^2 & -S^2 \\
 & & & & -S^2 & 1+2S^2
\end{bmatrix}
$$

$$
N \quad
\begin{bmatrix}
1 & & & & & \\
 & 1 & & & & \\
 & & 1 & & & \\
 & & & 1 & & \\
 & & & & 1 & \\
 & & & & & 1
\end{bmatrix}
\qquad
S = \frac{c\delta t}{\delta x} \gg 1
$$

Un-coupled system multiplying V^{n+1} & p^{n+1} separately

Substitution takes us from having to invert a 2N x 2N anti-symmetric system that has large off-diagonal elements to sequentially inverting a N x N symmetric system that is diagonally dominant + the identity matrix.

Mathematically equivalent → same answers! (but much better conditioned)

Relation of split implicit method to Schur Complement

The original system can be written as:

known RHS

$$\begin{bmatrix} \mathbf{A} & \mathbf{B} \\ \mathbf{C} & \mathbf{D} \end{bmatrix} \bullet \begin{bmatrix} \mathbf{V} \\ \mathbf{P} \end{bmatrix}^{n+1} = \begin{bmatrix} \mathbf{R} \\ \mathbf{Q} \end{bmatrix}^{n}$$

Here, $\mathbf{A}$ and $\mathbf{D}$ are diagonal matrices, and

$$\mathbf{B} = \begin{bmatrix} \cdots & & & & & \\ s & -s & & & & \\ & s & -s & & & \\ & & s & -s & & \\ & & & s & \cdots \end{bmatrix}, \quad \mathbf{C} = -\mathbf{B}^T = \begin{bmatrix} \cdots & & & & \\ & s & -s & & \\ & & s & -s & \\ & & & s & -s \\ & & & & \cdots \end{bmatrix}, \quad \mathbf{V} = \begin{bmatrix} \cdots \\ V_{j-1} \\ V_j \\ V_{j+1} \\ \cdots \end{bmatrix}, \quad \mathbf{P} = \begin{bmatrix} \cdots \\ p_{j-1/2} \\ p_{j+1/2} \\ p_{j+3/2} \\ \cdots \end{bmatrix}.$$

Solve first for $\mathbf{P}^{n+1}$ in terms of $\mathbf{V}^{n+1}$: $\mathbf{P}^{n+1} = -\, \mathbf{D}^{-1}\, \mathbf{C}\, \mathbf{V}^{n+1} + \mathbf{D}^{-1}\, \mathbf{Q}^{n}$

Next, eliminate $\mathbf{P}^{n+1}$: $\mathbf{A}'\,\mathbf{V}^{n+1} = \mathbf{R}'^{n}$

$$\mathbf{A}' = \mathbf{A} - \mathbf{B}\,\mathbf{D}^{-1}\mathbf{C}$$

$$\mathbf{R}'^{n} = \mathbf{R}^{n} - \mathbf{B}\,\mathbf{D}^{-1}\mathbf{Q}^{n}$$

In this example, $\mathbf{A}'$ is symmetric

Now apply this technique to the basic 3D MHD equations:

$$\left.\begin{aligned}
\rho_0 \dot{\mathbf{V}} &= \frac{1}{\mu_0}\left[\nabla\times\mathbf{B}\right]\times\mathbf{B} - \nabla p \\
\dot{\mathbf{B}} &= \nabla\times\left[\mathbf{V}\times\mathbf{B}\right] \\
\dot{p} &= -\mathbf{V}\bullet\nabla p - \gamma p \nabla\bullet\mathbf{V}
\end{aligned}\right\}$$

Ideal MHD Equations for velocity, magnetic field, and pressure:

Symmetric Hyperbolic System

7-waves

$$\begin{aligned}
\rho_0 \dot{\mathbf{V}} &= \frac{1}{\mu_0}\left[\nabla\times\left(\mathbf{B}+\theta\delta t\dot{\mathbf{B}}\right)\right]\times\left(\mathbf{B}+\theta\delta t\dot{\mathbf{B}}\right) - \nabla\left(p+\theta\delta t\dot{p}\right) \\
\dot{\mathbf{B}} &= \nabla\times\left[\left(\mathbf{V}+\theta\delta t\dot{\mathbf{V}}\right)\times\mathbf{B}\right] \\
\dot{p} &= -\left(\mathbf{V}+\theta\delta t\dot{\mathbf{V}}\right)\bullet\nabla p - \gamma p \nabla\bullet\left(\mathbf{V}+\theta\delta t\dot{\mathbf{V}}\right)
\end{aligned}$$

Taylor Expand in Time

Substitute from 2nd and 3rd equation into first, finite difference in time:

$$\left\{\rho - \theta^2(\delta t)^2 L\right\}\mathbf{V}^{n+1} = \left\{\rho - \theta^2(\delta t)^2 L\right\}\mathbf{V}^{n} + \delta t\left\{-\nabla p + \frac{1}{\mu_0}(\nabla\times\mathbf{B})\times\mathbf{B}\right\}^{n}$$

MHD Operator: $\longrightarrow$

$$\begin{aligned}
L\{\mathbf{V}\} = {}& \frac{1}{\mu_0}\left\{\nabla\times\left[\nabla\times\left(\mathbf{V}\times\mathbf{B}\right)\right]\right\}\times\mathbf{B} + \frac{1}{\mu_0}\left(\nabla\times\mathbf{B}\right)\times\left[\nabla\times\left(\mathbf{V}\times\mathbf{B}\right)\right] \\
& + \nabla\left(\mathbf{V}\bullet\nabla p + \gamma p \nabla\bullet\mathbf{V}\right)
\end{aligned}$$

3 step physics-based preconditioner greatly improves iterative solve

(1) Split implicit formulation

(2) Apply annihilation operators

(3) Apply block-Jacobi preconditioner by using SuperLU_dist on each poloidal plane independently

Original matrix multiplying
$\mathbf{V}^{n+1}$, $\mathbf{B}^{n+1}$, p^{n+1}
- non-symmetric,
- non-diagonally dominant &
- large range of eigenvalues

→ → → → GMRES

Smaller matrix multiplying $\mathbf{V}^{n+1}$ only,
- nearly symmetric
- closer to diagonal
- still with large range of eigenvalues

Matrix now consists of 3 dominant diagonal blocks, each with narrower range of eigenvalues.

Now, range of eigenvalues in each block is greatly reduced.

Preconditioned system converges in 10’s of iterations

(2) Apply annihilation operators to separate eigenvalues into diagonal blocks

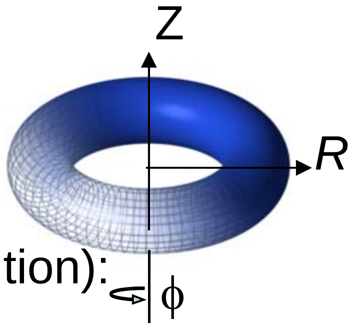

Velocity vector written in terms of 3 scalar fields (Helmholtz decomposition):

$$\mathbf{V} = R^2 \nabla U \times \nabla \phi + R^2 \omega \nabla \phi + \frac{1}{R^2} \nabla_\perp \chi$$

$$\nabla_\perp \equiv \hat{R}\frac{\partial}{\partial R} + \hat{Z}\frac{\partial}{\partial Z}$$

Associated mainly with the shear Alfven wave: does not compress the toroidal field

Associated mainly with the slow wave: also does not compress the toroidal field

Associated mainly with the fast wave: does compress the toroidal field

To obtain scalar equations, we apply annihilation projections to isolate the physics associated with the different wave types in different blocks in the matrix

Alfven wave: $\nabla \phi \bullet \nabla_\perp \times R^2$

slow wave: $R^2 \nabla \phi \bullet$

fast wave: $-\nabla_\perp \bullet R^{-2}$

$$\left(1 - \theta^2 (\delta t) L\right) \frac{\partial \mathbf{V}}{\partial t} + \mathbf{V} \bullet \nabla \mathbf{V} = \frac{1}{n M_i} \left[-\nabla p + \mathbf{J} \times \mathbf{B} - \nabla \bullet \mathbf{\Pi}_{GV} - \nabla \bullet \mathbf{\Pi}_\mu \right]$$

Code can be run with 1,2 (reduced MHD) or 3 (full MHD) velocity variables

Aside on the form of the Vector Fields

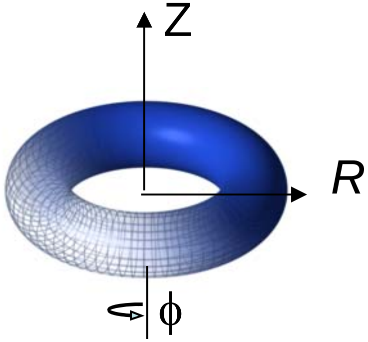

Because the externally imposed toroidal field in a tokamak is very strong, any plasma instability will slip through this field and not compress it. We need to be able to model this motion very accurately because of the weak forces causing the instability.

In **M3D-*C*[1]**, we express the velocity field as shown

$$\mathbf{V} = R^2 \nabla U \times \nabla \phi + R^2 \omega \nabla \phi + \frac{1}{R^2} \nabla_\perp \chi$$

All components orthogonal !

$$\int |\mathbf{V}|^2 d\tau = \int \left[R^2 |\nabla_\perp U|^2 + R^2 \omega^2 + \frac{1}{R^4} |\nabla_\perp \chi|^2 \right] d\tau$$

Consider now the action of the first term in $\mathbf{V}$ on the external toroidal field:

$$\mathbf{B} = F_0 \nabla \phi \qquad \mathbf{V} = R^2 \nabla U \times \nabla \phi$$

$$\begin{aligned} \nabla \phi \bullet \left[\frac{\partial \mathbf{B}}{\partial t} = \nabla \times (\mathbf{V} \times \mathbf{B}) \right] &= \nabla \phi \bullet \nabla \times \left[\left(R^2 \nabla U \times \nabla \phi \right) \times F_0 \nabla \phi \right] \\ &= -F_0 \nabla \bullet \left[\nabla U \times \nabla \phi \right] \\ &= 0 \end{aligned}$$

The velocity field U does not compress the external toroidal field!

- Any unstable motion will mostly consist of the velocity component U….
- Analytic elimination of this potentially stabilizing term greatly increases accuracy.

M3D-C^1 can be run with 1, 2, or 3 velocity variables. Tracking the eigenvalues shows how they separate into 3 groups in a cylinder

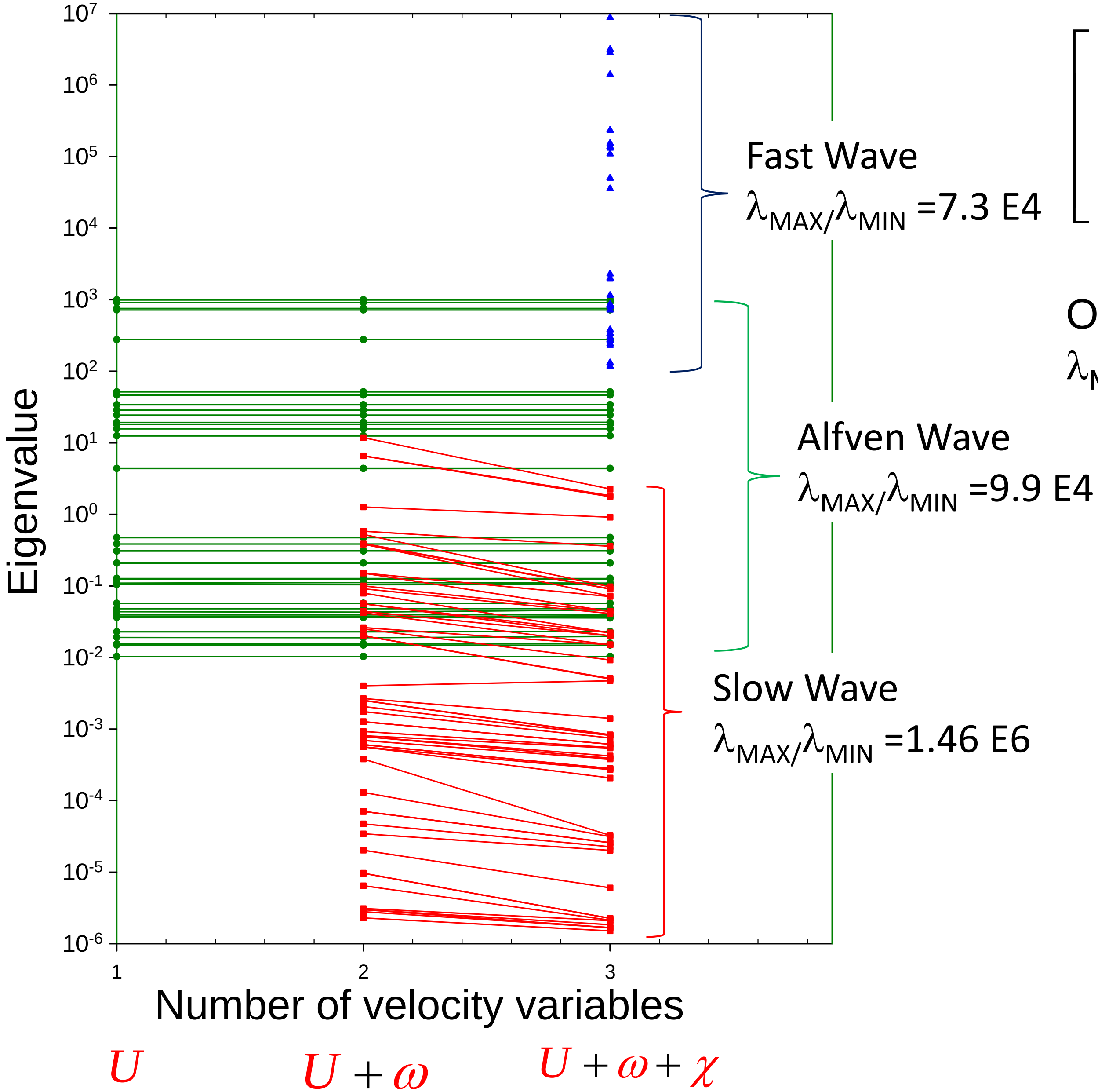

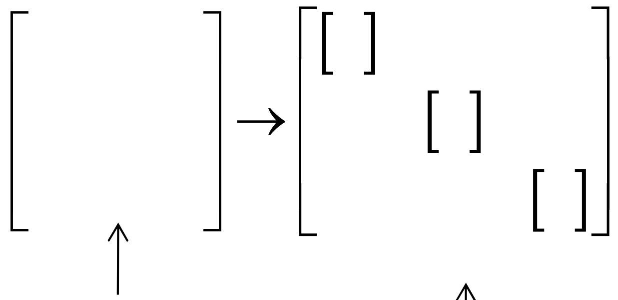

Original matrix:
$\lambda_{MAX}/\lambda_{MIN} = 10^{13}$

Annihilation operators split this into 3 loosely connected matrices, each with a condition number much less than original matrix

3 step physics-based preconditioner greatly improves iterative solve

(1) Split implicit formulation

(2) Apply annihilation operators

(3) Apply block-Jacobi preconditioner by using SuperLU_dist on each poloidal plane independently

Original matrix multiplying
$\mathbf{V}^{n+1}$, $\mathbf{B}^{n+1}$, p^{n+1}
- non-symmetric,
- non-diagonally dominant &
- large range of eigenvalues

→ [ ] → [[ ] [ ] [ ]] → [[ ] [ ] [ ]] → GMRES

Smaller matrix multiplying $\mathbf{V}^{n+1}$ only,
- nearly symmetric
- closer to diagonal
- still with large range of eigenvalues

Matrix now consists of 3 dominant diagonal blocks, each with narrower range of eigenvalues.

Now, range of eigenvalues in each block is greatly reduced.

Preconditioned system converges in 10's of iterations

(3) Apply block-Jacobi preconditioner by using SuperLU_dist on each poloidal plane independently

M3D-C^1 uses a triangular wedge high order finite element

- Continuous 1st derivatives in all directions … *C^1 continuity*
- Unstructured triangles in (R,Z) plane
- Structured in toroidal direction (φ)

Triangular wedge integration volume

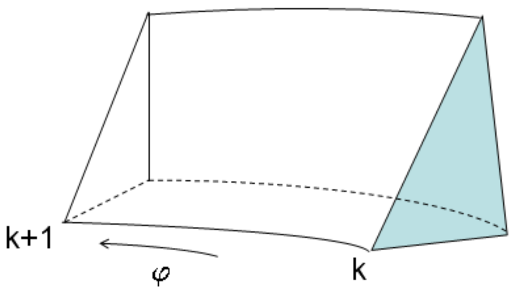

Top view: 16-32 toroidal prisms

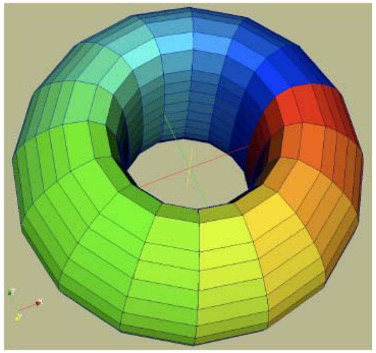

Slice view: ~ 10^4 nodes/plane

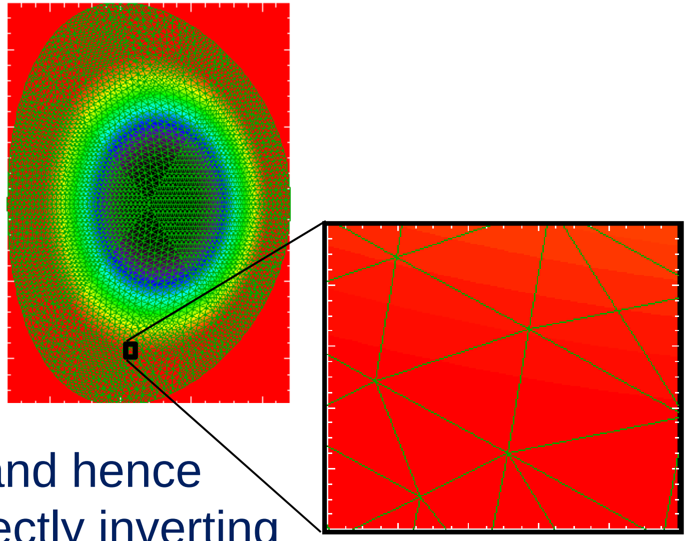

Because of the small zone size within the plane, and hence strong coupling, we precondition the matrix by directly inverting the components within each poloidal plane simultaneously.

Block Jacobi Preconditioner: greatly reduces condition number

(3) Apply block-Jacobi preconditioner by using SuperLU_dist on each poloidal plane independently (cont)

- All the nodes on each poloidal plane are coupled only to their nearest neighbors. This leads to block triangular structure

$$\begin{bmatrix} B_1 & C_1 & & & & & & A_1 \\ \bullet & \bullet & \bullet & & & & & \\ & \bullet & \bullet & \bullet & & & & \\ & & A_j & B_j & C_j & & & \\ & & & \bullet & \bullet & \bullet & & \\ & & & & \bullet & \bullet & \bullet & \\ & & & & & \bullet & \bullet & \bullet \\ C_N & & & & & & A_N & B_N \end{bmatrix} \bullet \begin{bmatrix} V_1 \\ \cdot \\ V_{j-1} \\ V_j \\ V_{j+1} \\ \cdot \\ \cdot \\ V_N \end{bmatrix}^{n+1} = \begin{bmatrix} y_1 \\ \cdot \\ y_{j-1} \\ y_j \\ y_{j+1} \\ \cdot \\ \cdot \\ y_N \end{bmatrix}^{n}$$

A_j, B_j, C_j are 2D sparse matrices at plane j

V_j denotes all the velocity variables on plane j

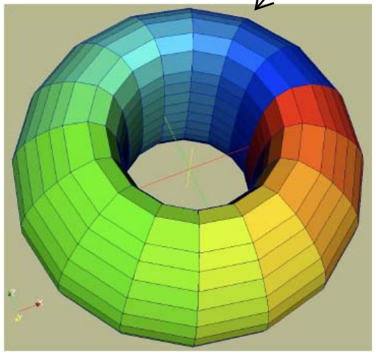

Block Jacobi preconditioner corresponds to multiplying each row by inverse of diagonal block B_j^{-1}

PETSc now has the capability of doing this using SuperLU_Dist or MUMPS concurrently on each plane

Eigenvalues of A=3 3D Matrix

Before and **After** Preconditioning

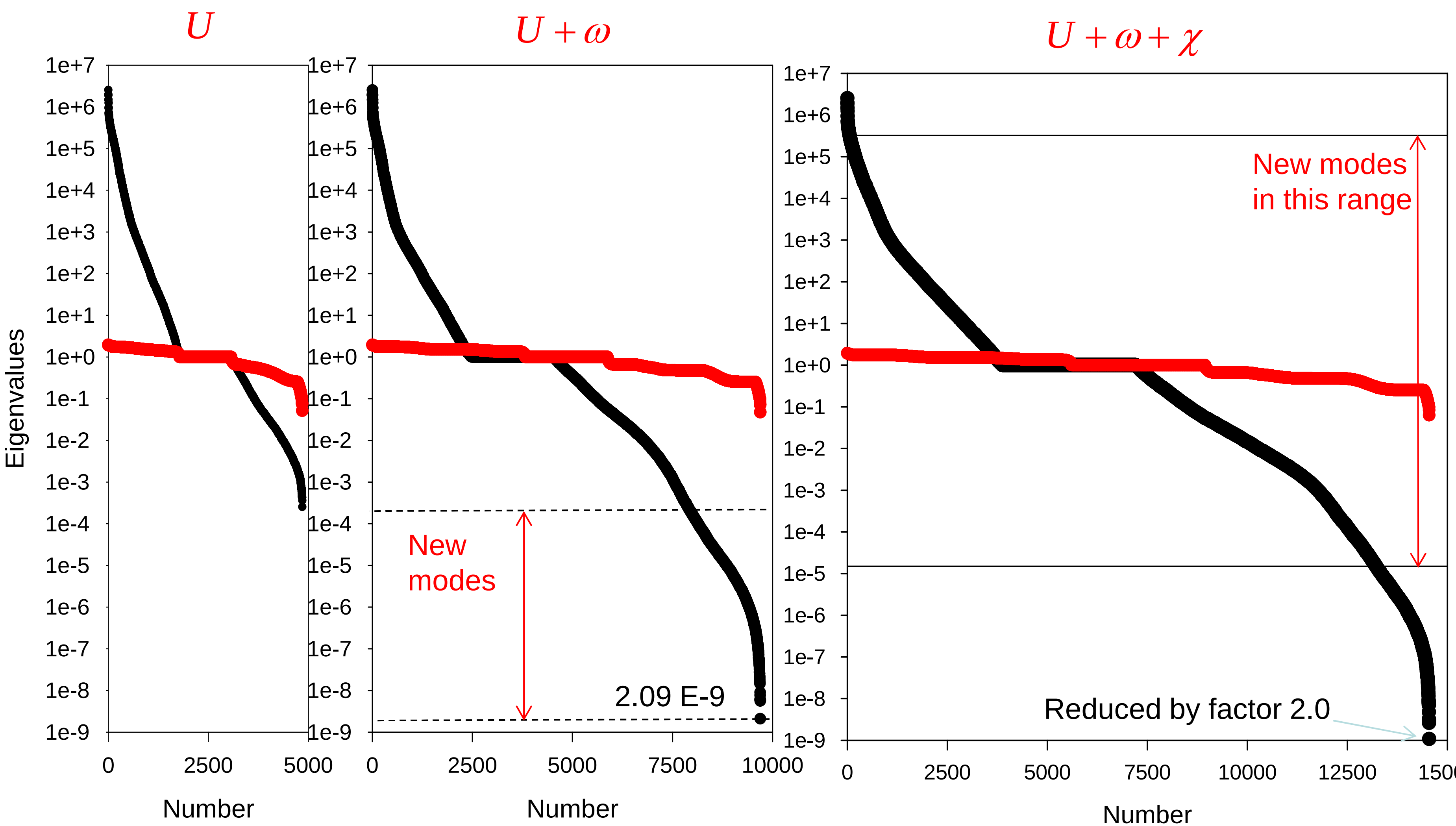

Extensive benchmarking for ideal, resistive, and two fluid modes

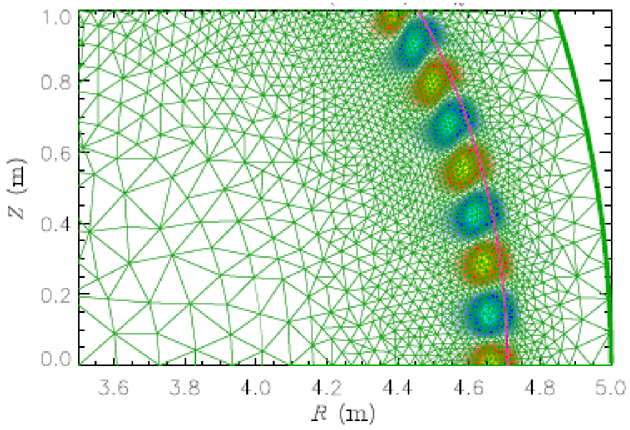

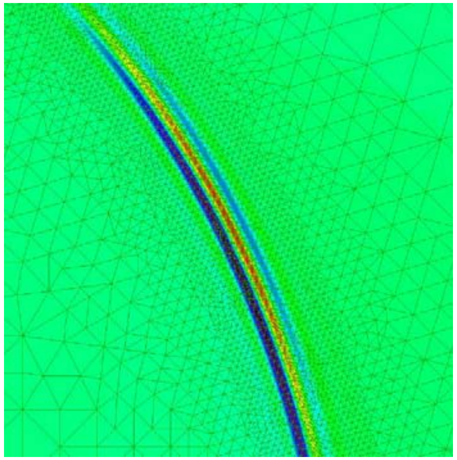

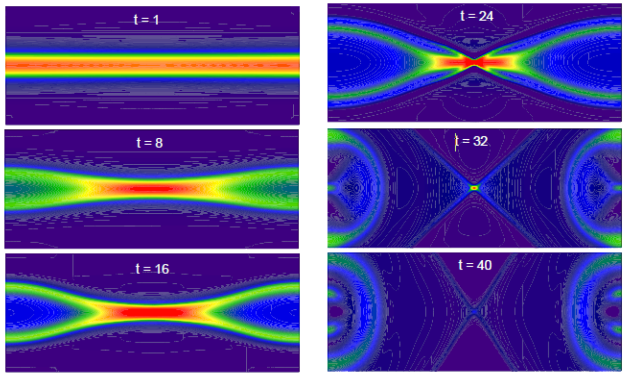

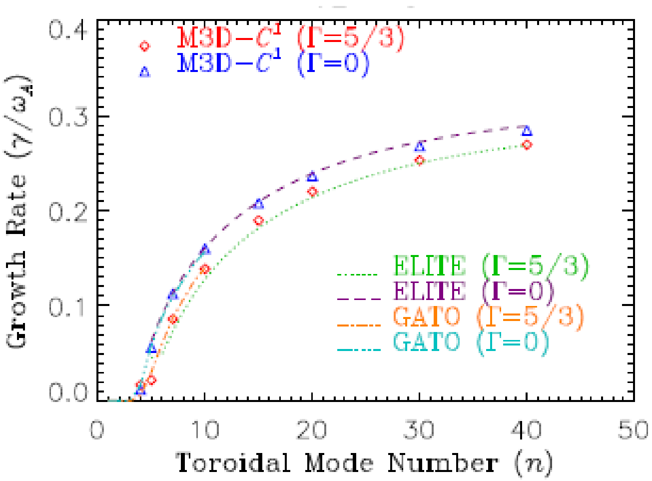

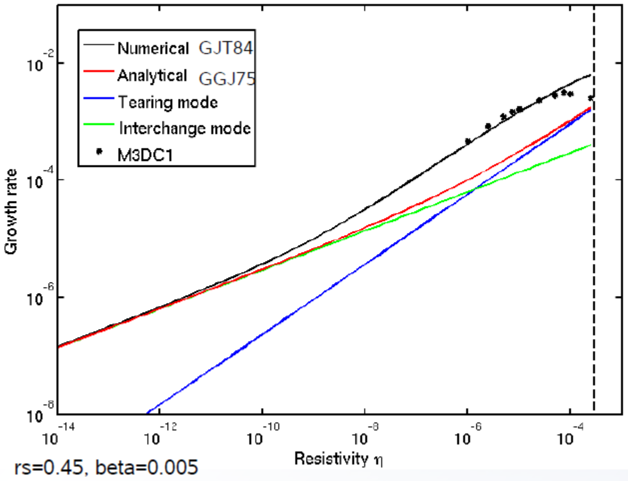

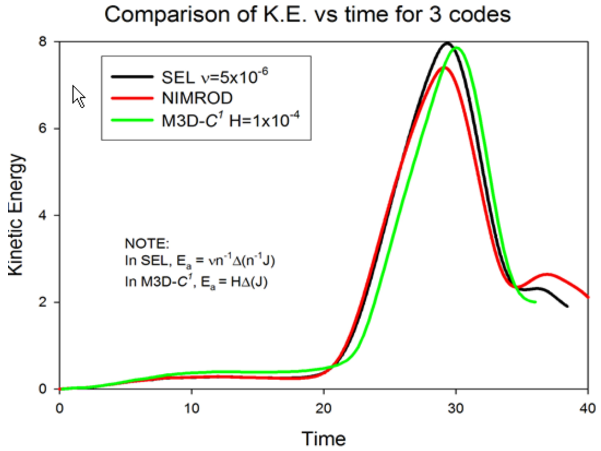

Ideal MHD

Resistive MHD

2-Fluid Reconnection

Parallel Scaling Studies have been performed from 96 to 12288 p

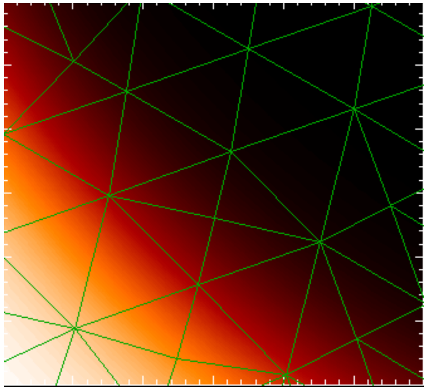

.08

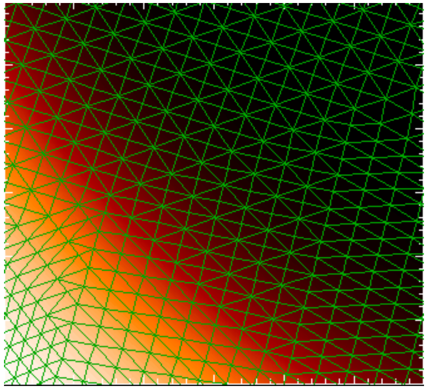

.02

Triangle linear dimension varied by factor of 4

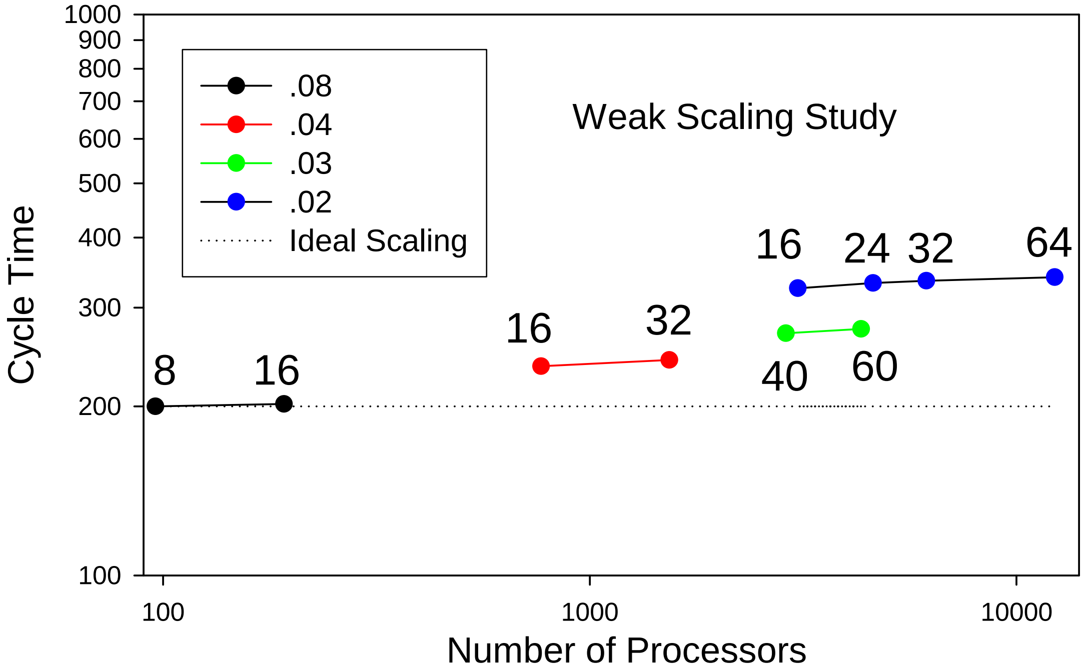

Number of toroidal planes varied from 8 to 64

Time increased by 1.7 as # of zones increased by 130

Transport Timescale simulations in which stability is important: with $\Delta t = 40\ \tau_A$

Specify a transport model:

Resistivity: $\eta = n^{3/2} p^{-3/2}$

Thermal Conductivity: $\kappa_\perp = n^{3/2} p^{-1/2}$

$$\kappa_\parallel = 10^6 \kappa_\perp$$

Viscosity: uniform (~η)

Current controller provides loop voltage to maintain plasma current at initial value.

Loop voltage provides thermal energy through Ohmic heating

Current density periodically peaks, becomes unstable, reconnects, and broadens…periodic cycle (sawtooth)

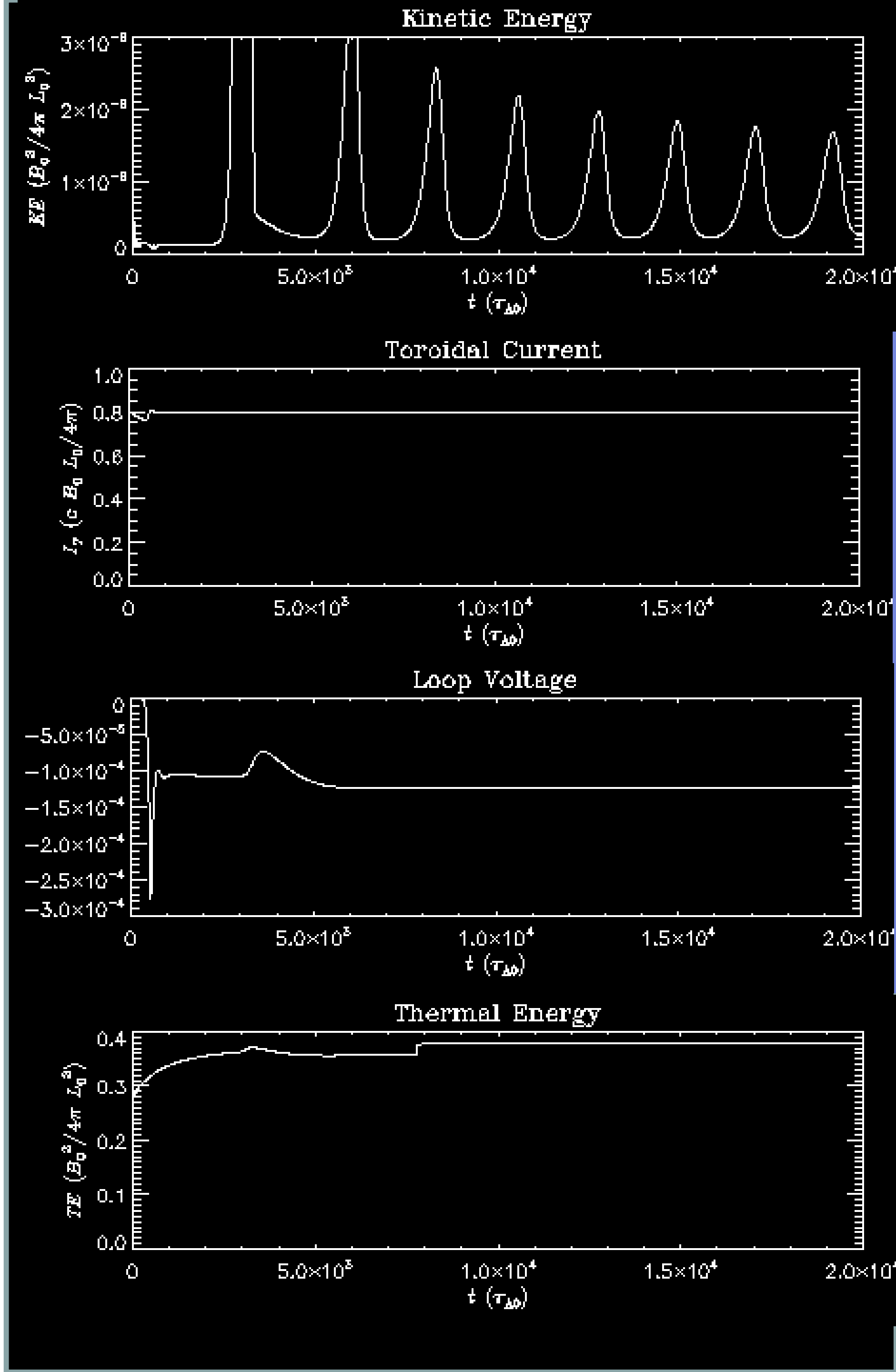

Generic sawtooth studies are now underway

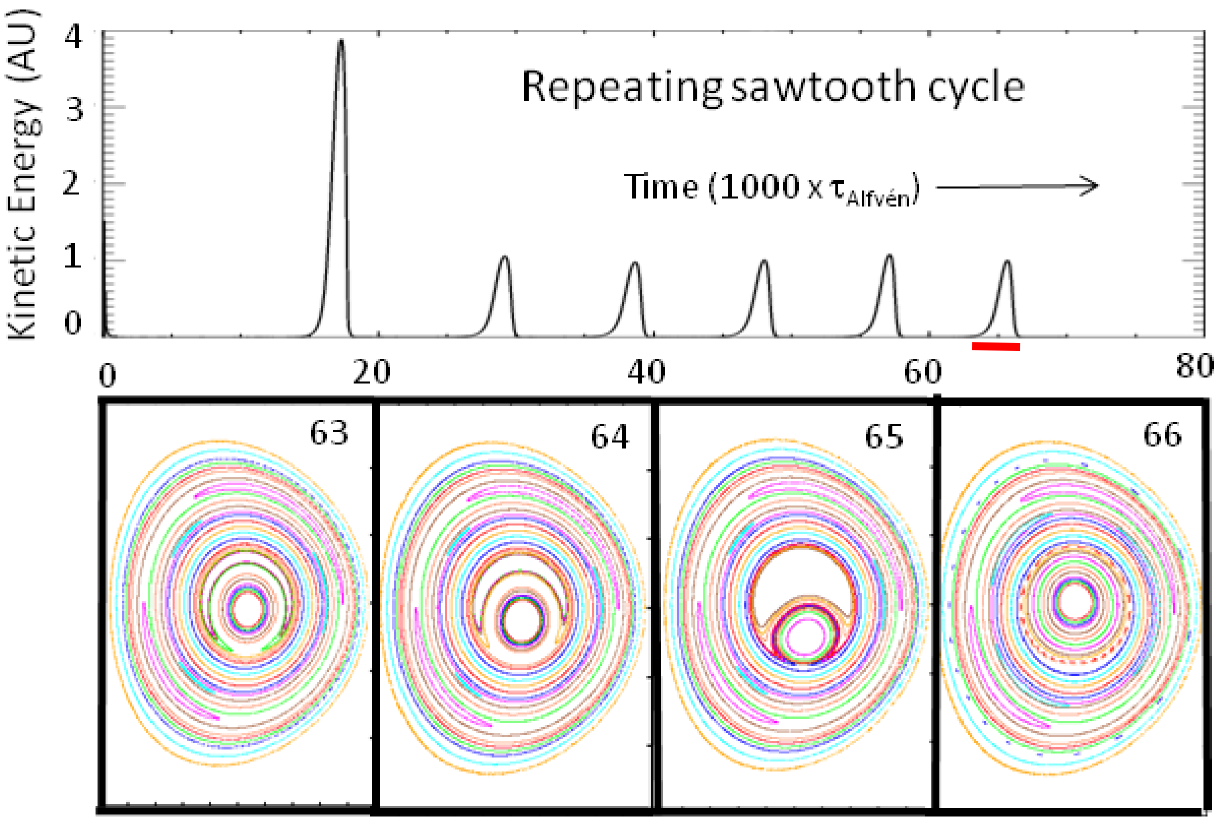

Typical result: 1st sawtooth event depends on initial conditions.
After many events, system reaches steady-state or periodic behavior

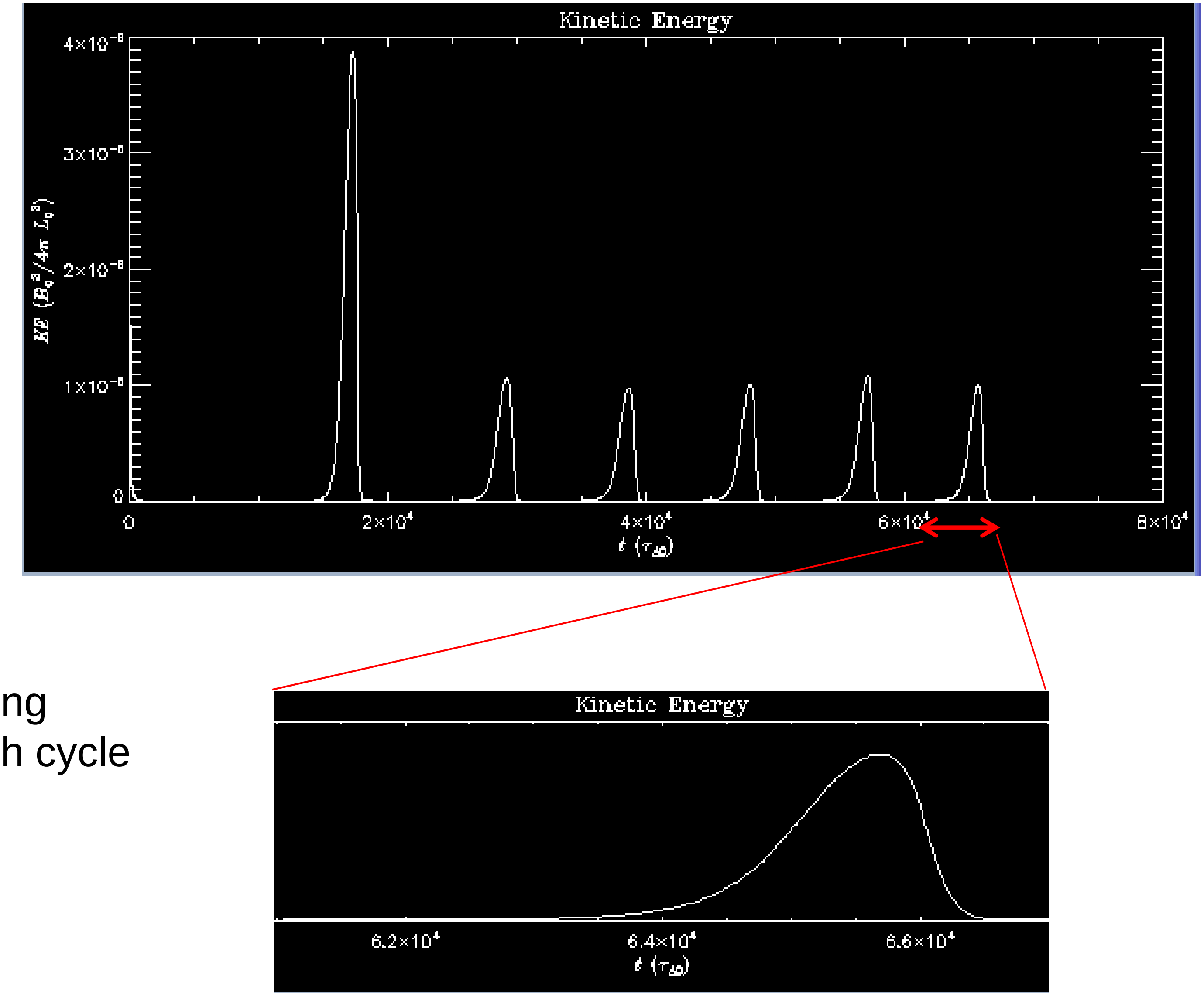

Repeating sawtooth cycle

Precursor phase Crash phase

Poincare plots during a single sawtooth cycle

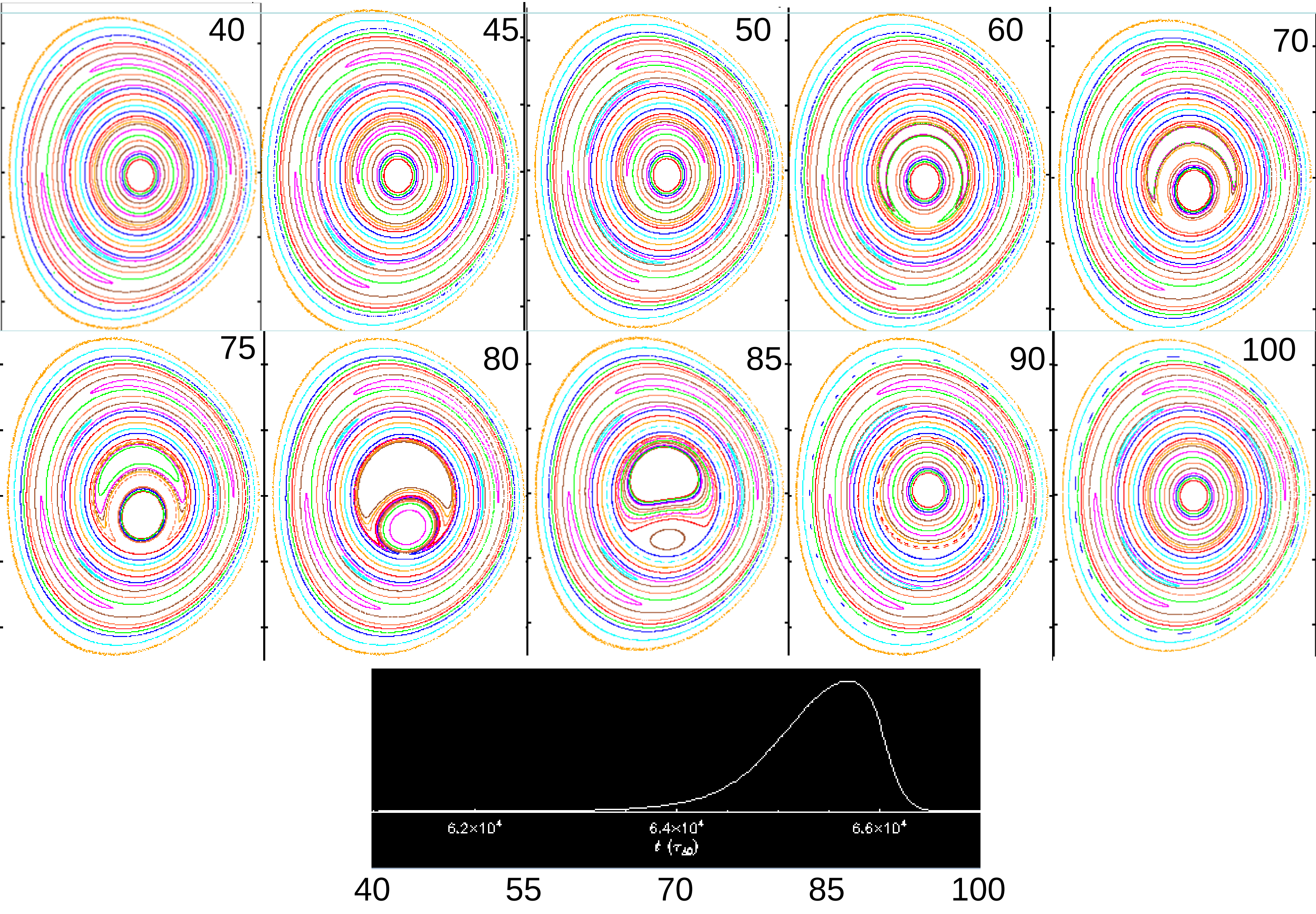

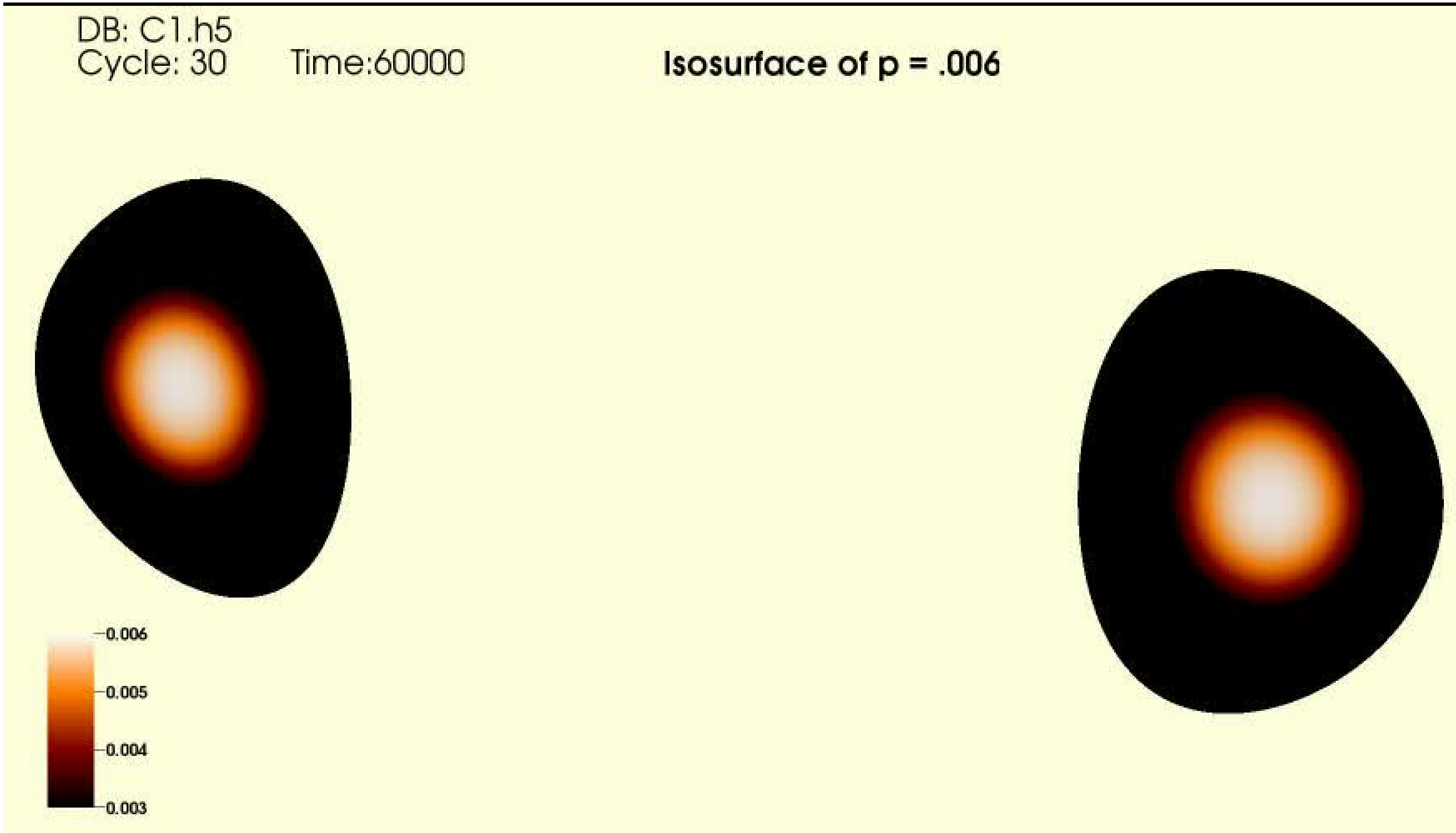
DB: C1.h5
Cycle: 30
Time:60000
Isosurface of p = .006
0.006
0.005
0.004
0.003

$$\mathbf{V} = R^2 \nabla U \times \nabla \phi + R^2 \omega \nabla \phi + \frac{1}{R^2} \nabla_\perp \chi$$

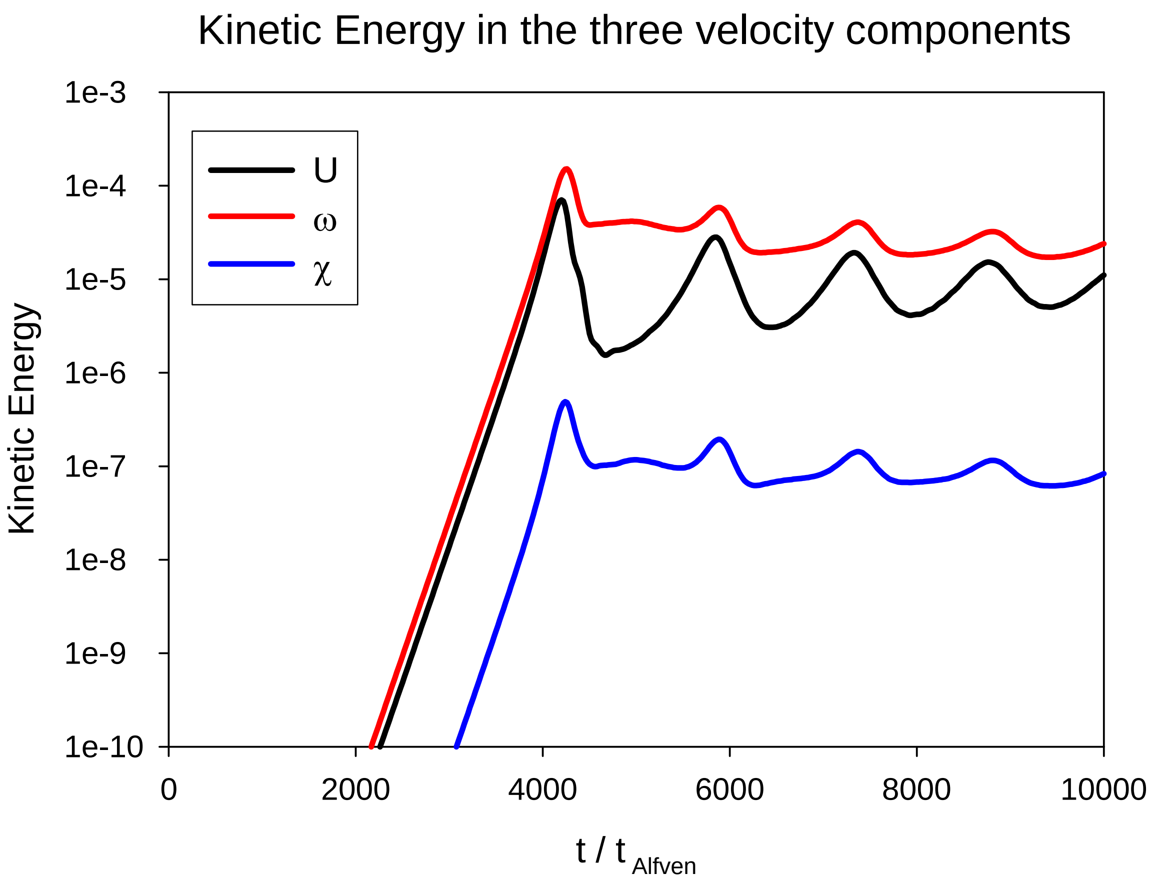

The poloidal velocity decomposition used in M3D-*C*[1] is very effective in capturing most of the poloidal flow in U.

Stationary States with Flow

In lower viscosity cases, the sawtooth behavior stops after a few cycles, and a central helical (1,1) structure forms with flow.

This flow is such as to flatten the central pressure and temperature. This flattening causes the current density to also flatten near the center, keeping $q_0 \sim 1$ in the central region.

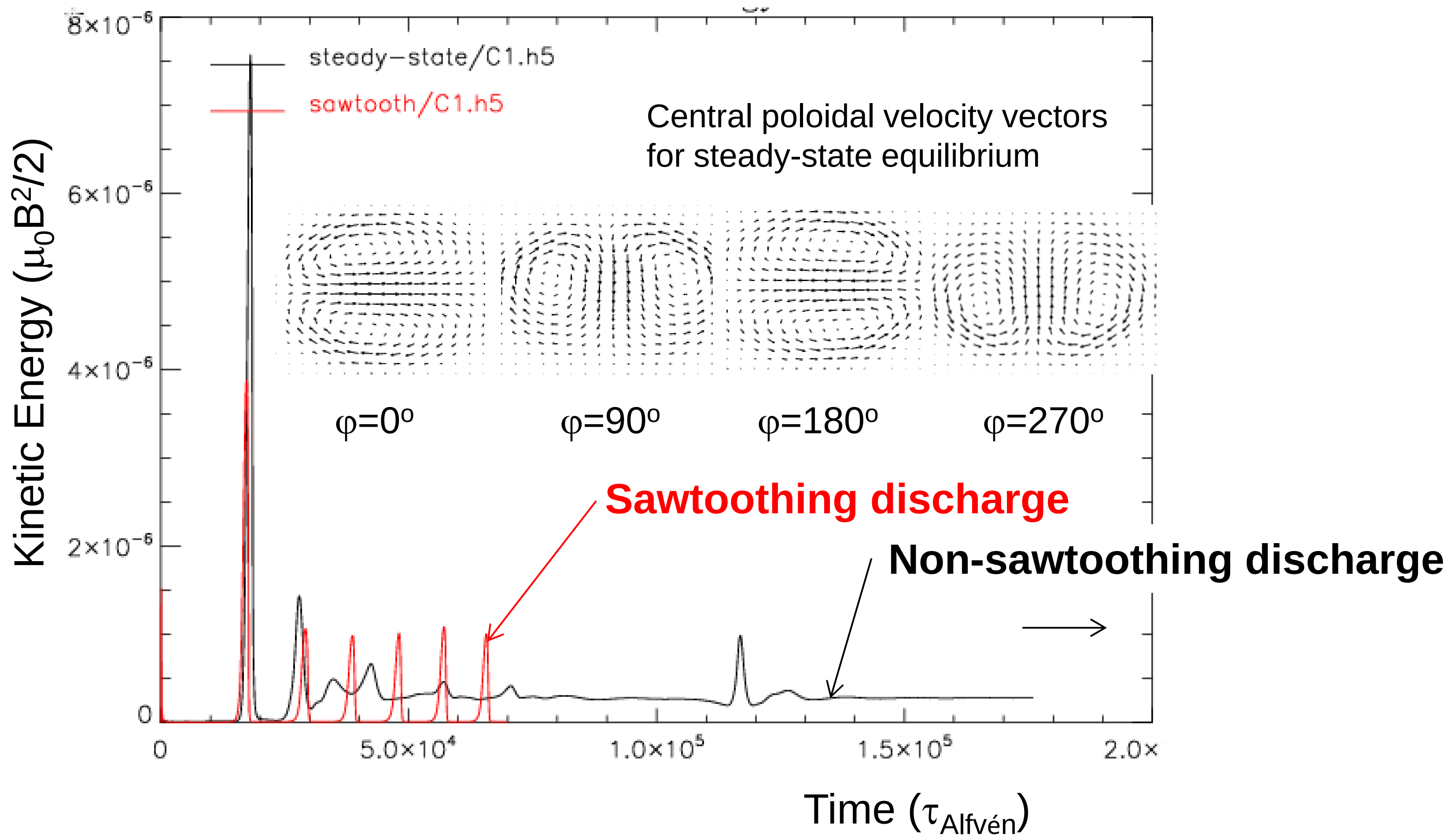

8×10⁻⁶
6×10⁻⁶
4×10⁻⁶
2×10⁻⁶
0
steady-state/C1.h5
sawtooth/C1.h5
Central poloidal velocity vectors
for steady-state equilibrium
φ=0º
φ=90º
φ=180º
φ=270º
Sawtoothing discharge
Non-sawtoothing discharge
0
5.0×10⁴
1.0×10⁵
1.5×10⁵
2.0×
Kinetic Energy ($\mu_0 B^2/2$)
Time ($\tau_{Alfvén}$)

Comparison of 3D Sawtooth Free Helical Stationary State (SFHSS) with 2D configuration with same transport parameters

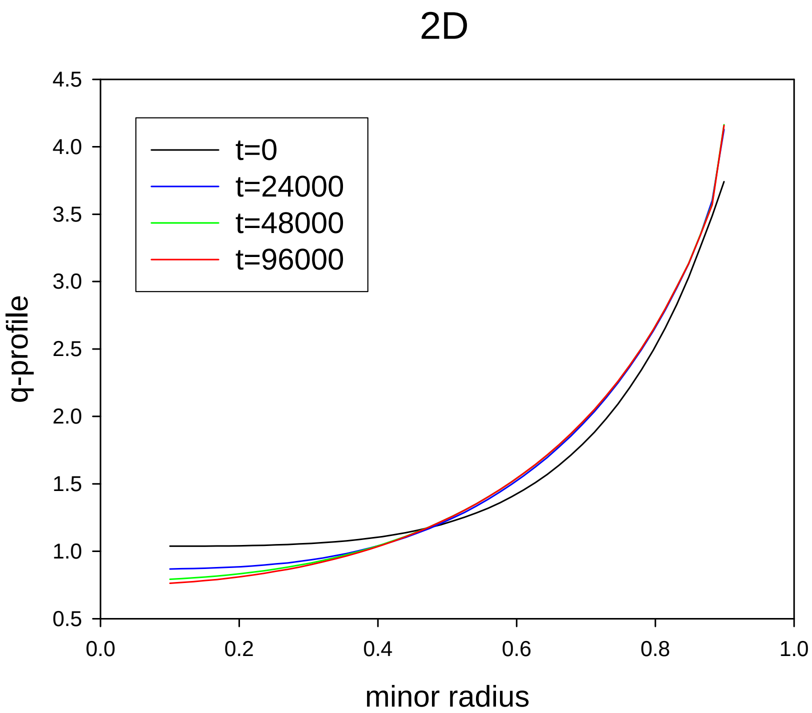

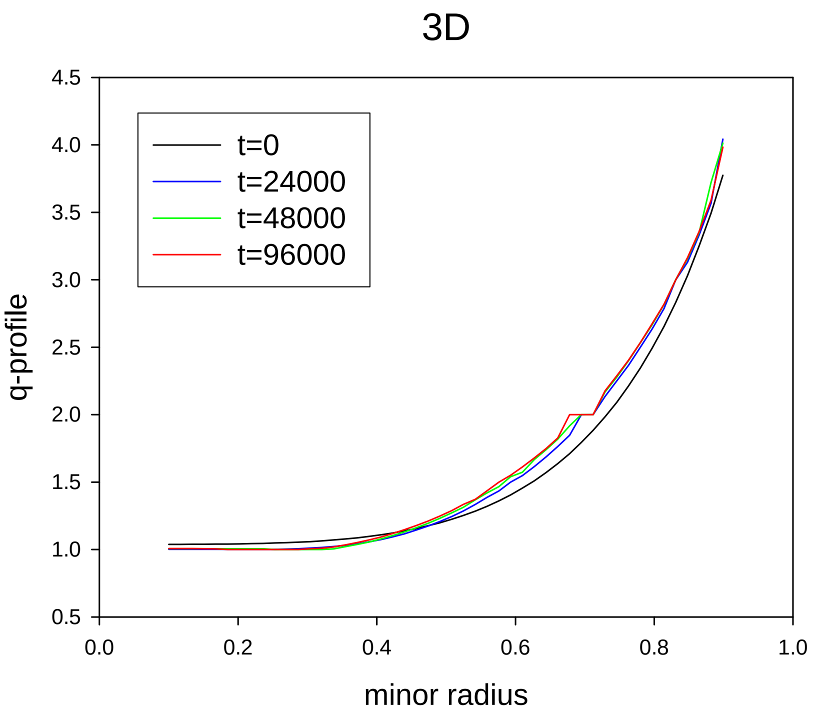

Exact same case was run with M3D-C^1 in 2D and in 3D.

- In 2D, q_0 drops to about 0.7.
- In 3D, it is clamped at 1.0

Comparison of 3D Sawtooth Free Helical Stationary State (SFHSS) with 2D configuration with same transport parameters

2D 3D

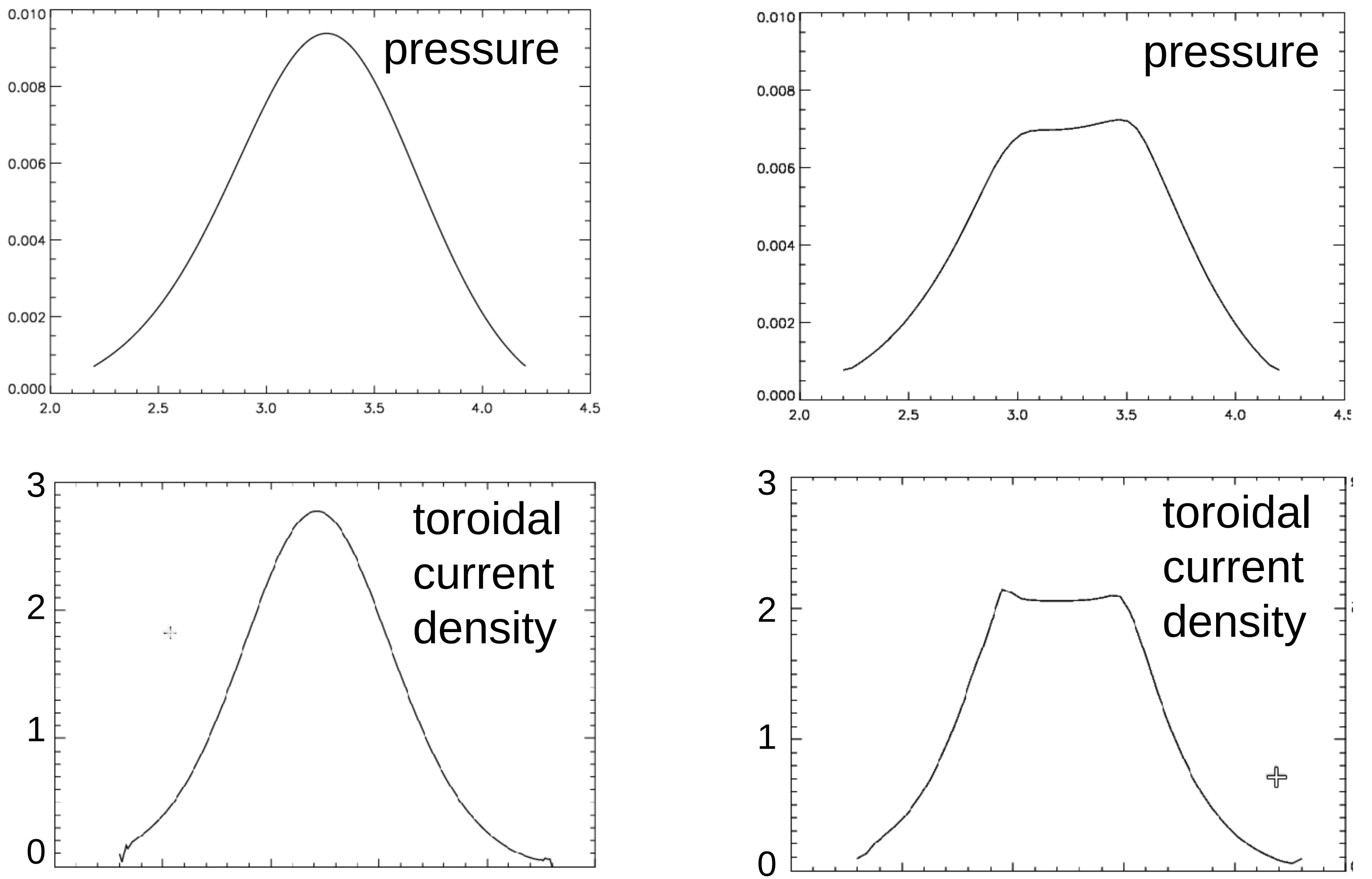

In 3D, pressure and toroidal current density are much less peaked.

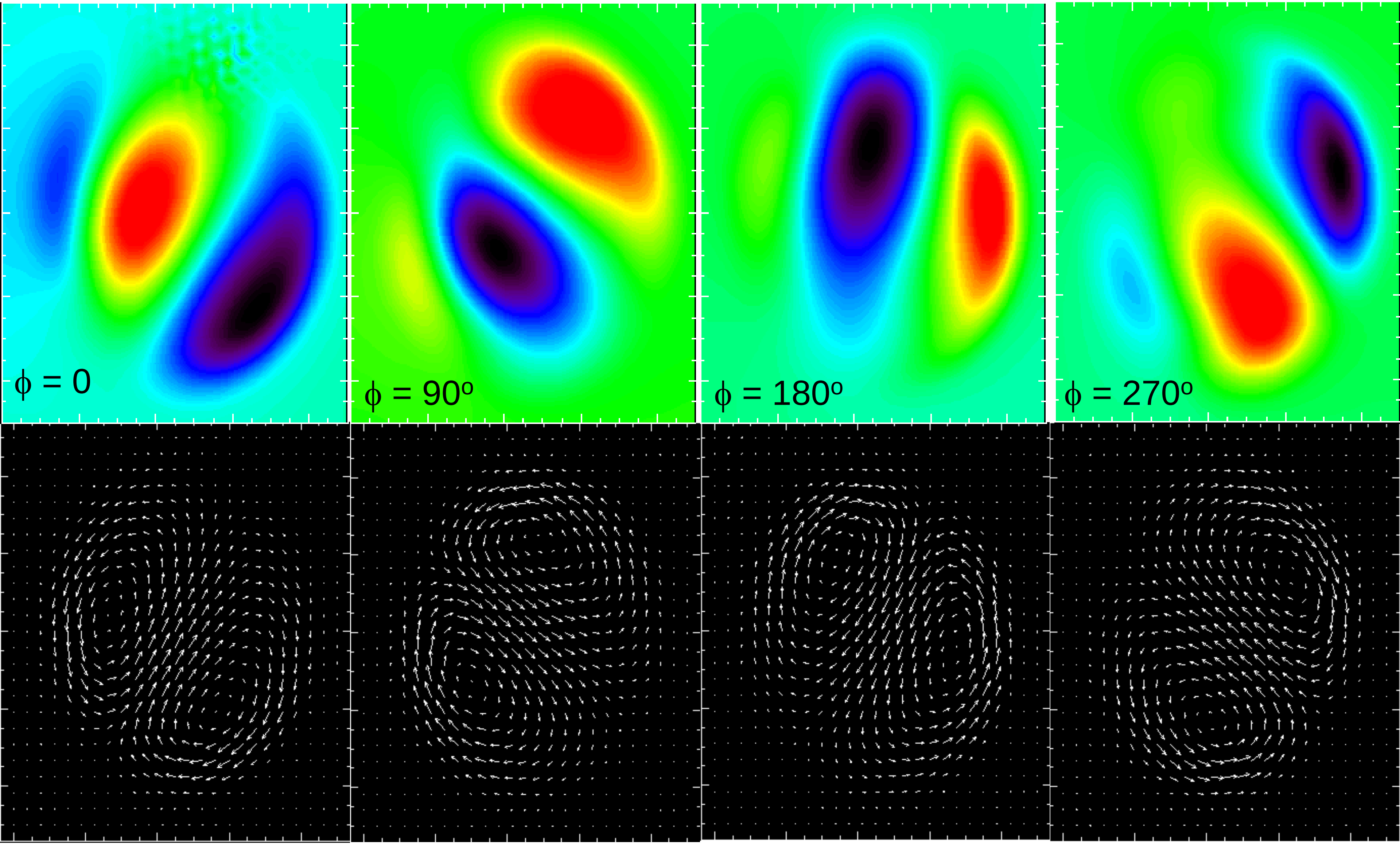

Close up of central toroidal velocity contours (top) and poloidal velocity vectors for stationary state at different toroidal angles: $V_T(max) \sim 0.0004$, $V_P(max) \sim 0.0002$

Differences in sawtooth behavior for bean-shaped and elliptical-shaped plasmas has been well documented experimentally (Lazarus, Tobias, …)

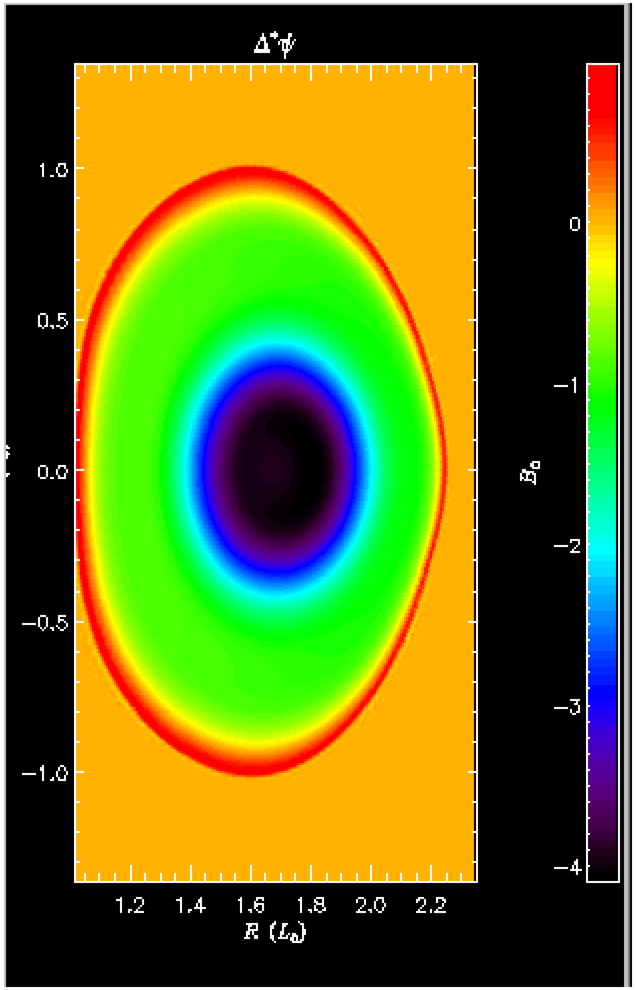

DIII-D shot 118164

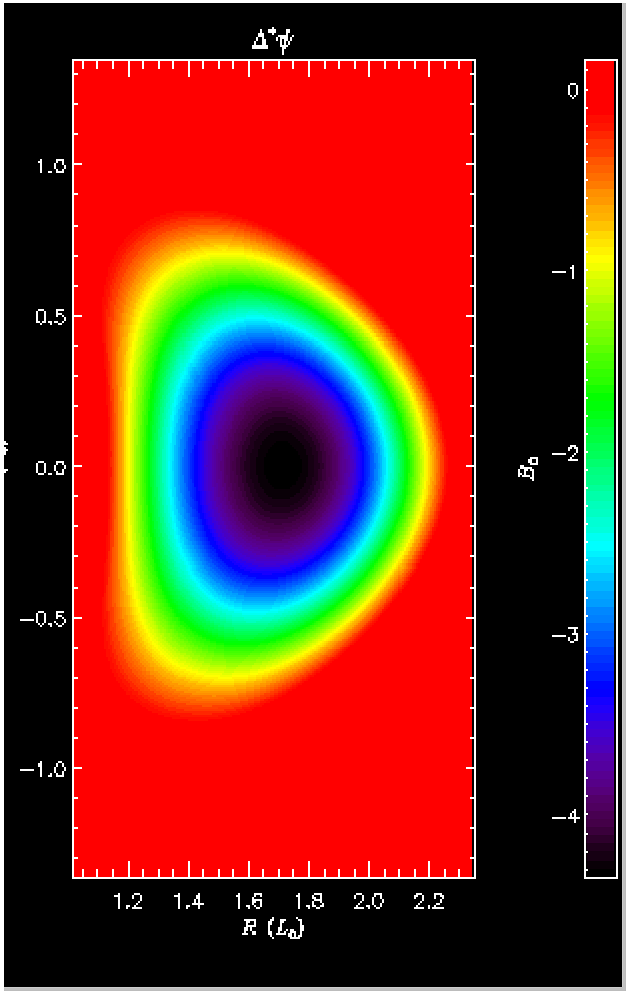

DIII-D shot 118162

We have imported these equilibria from geqdsk files, and inferred the transport properties from the plasma properties…simulations in progress

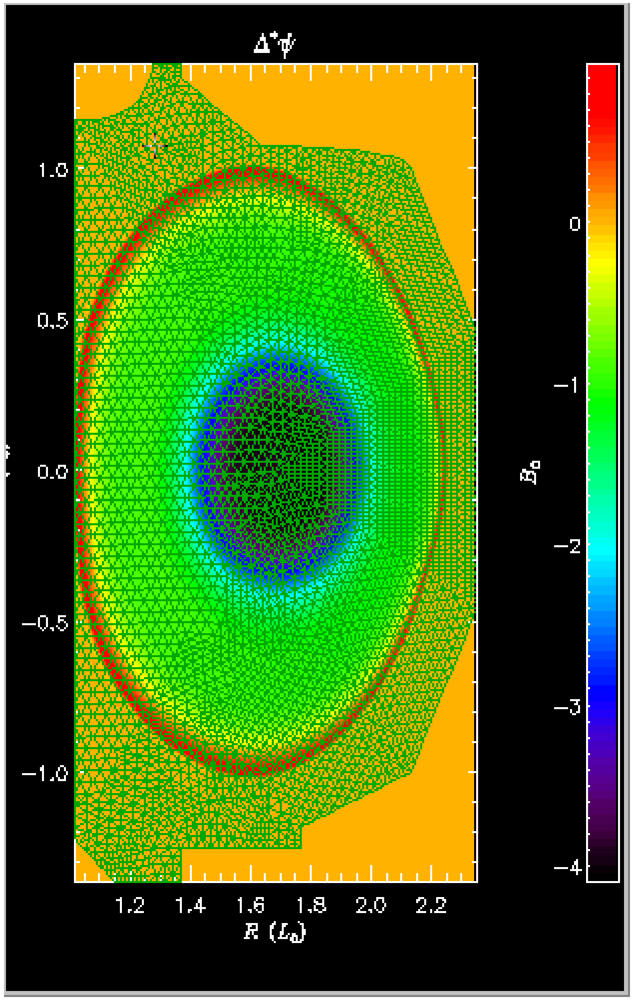

DIII-D shot 118164

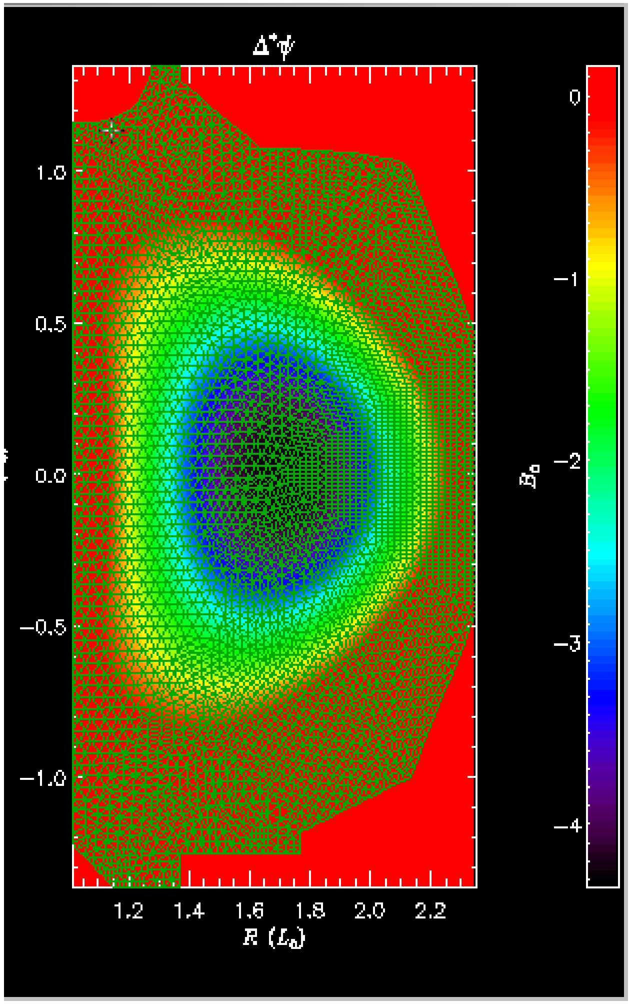

DIII-D shot 118162

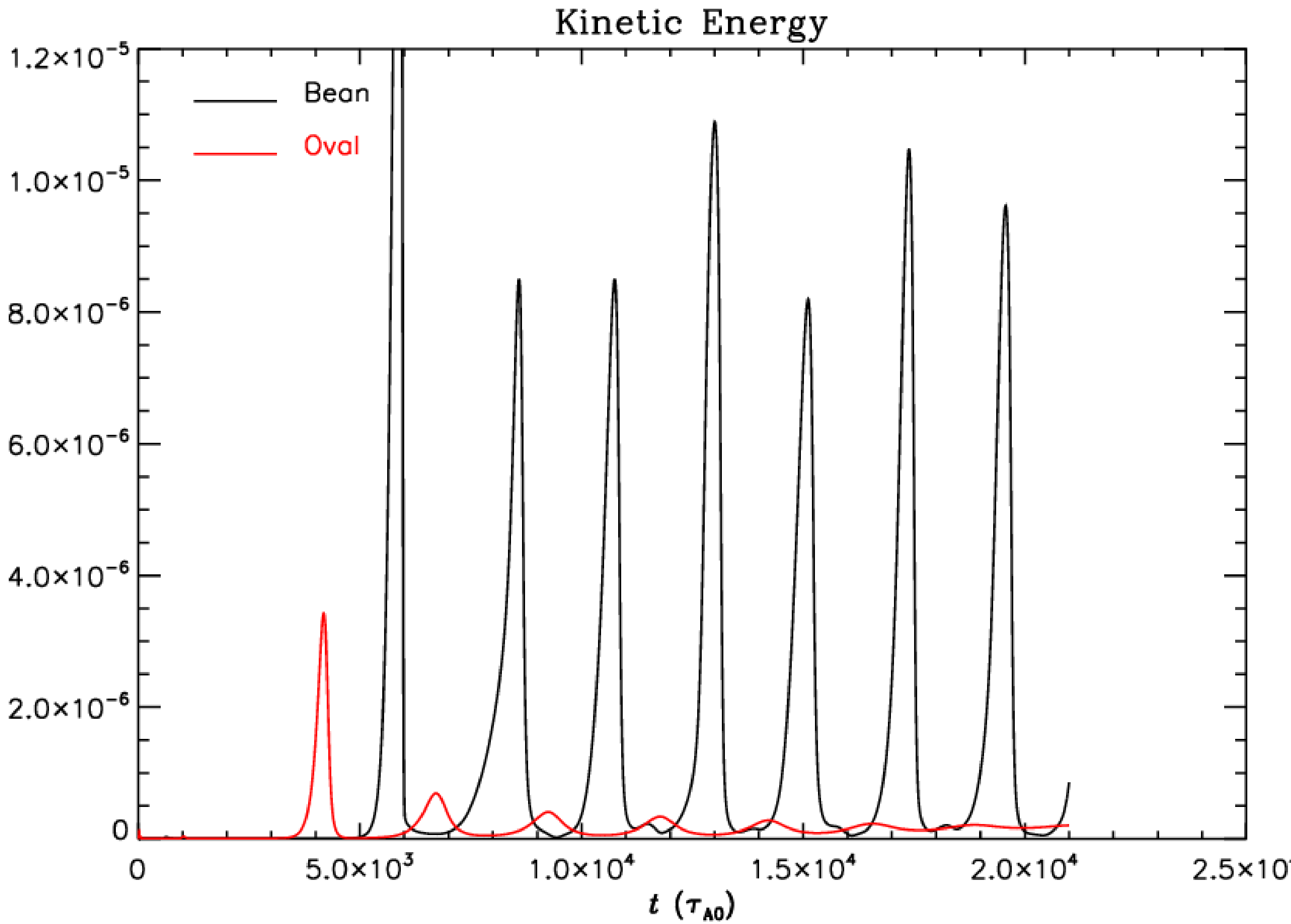
Kinetic Energy
Bean
Oval
1.2×10⁻⁵
1.0×10⁻⁵
8.0×10⁻⁶
6.0×10⁻⁶
4.0×10⁻⁶
2.0×10⁻⁶
0
0
5.0×10³
1.0×10⁴
1.5×10⁴
2.0×10⁴
2.5×10⁴
t (τA0)

Stationary Pressure for DIII-D Oval (shot 118164)

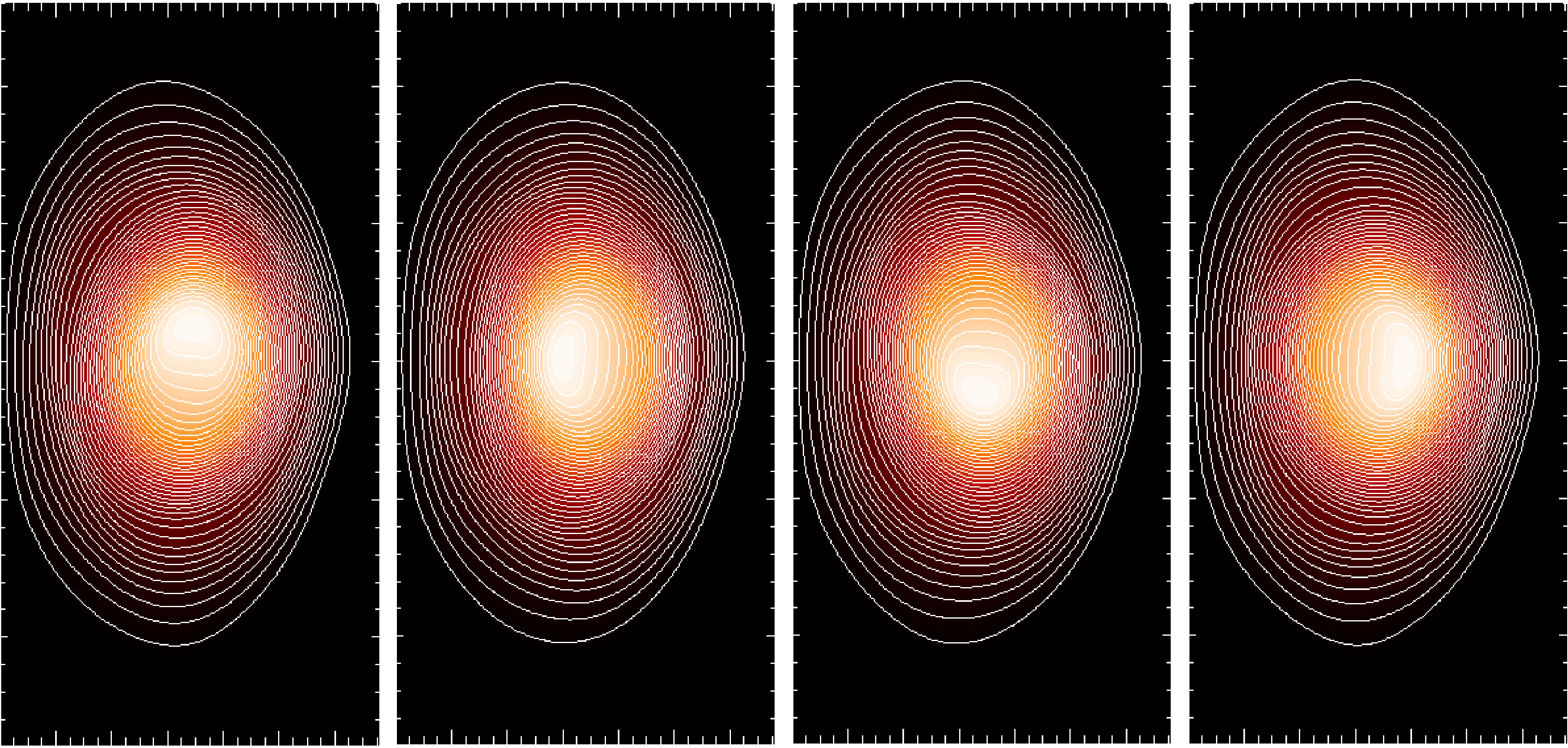

$\varphi = 0^o$ $\varphi = 90^o$ $\varphi = 180^o$ $\varphi = 270^o$

Stationary Current Density for DIII-D Oval (shot 118164)

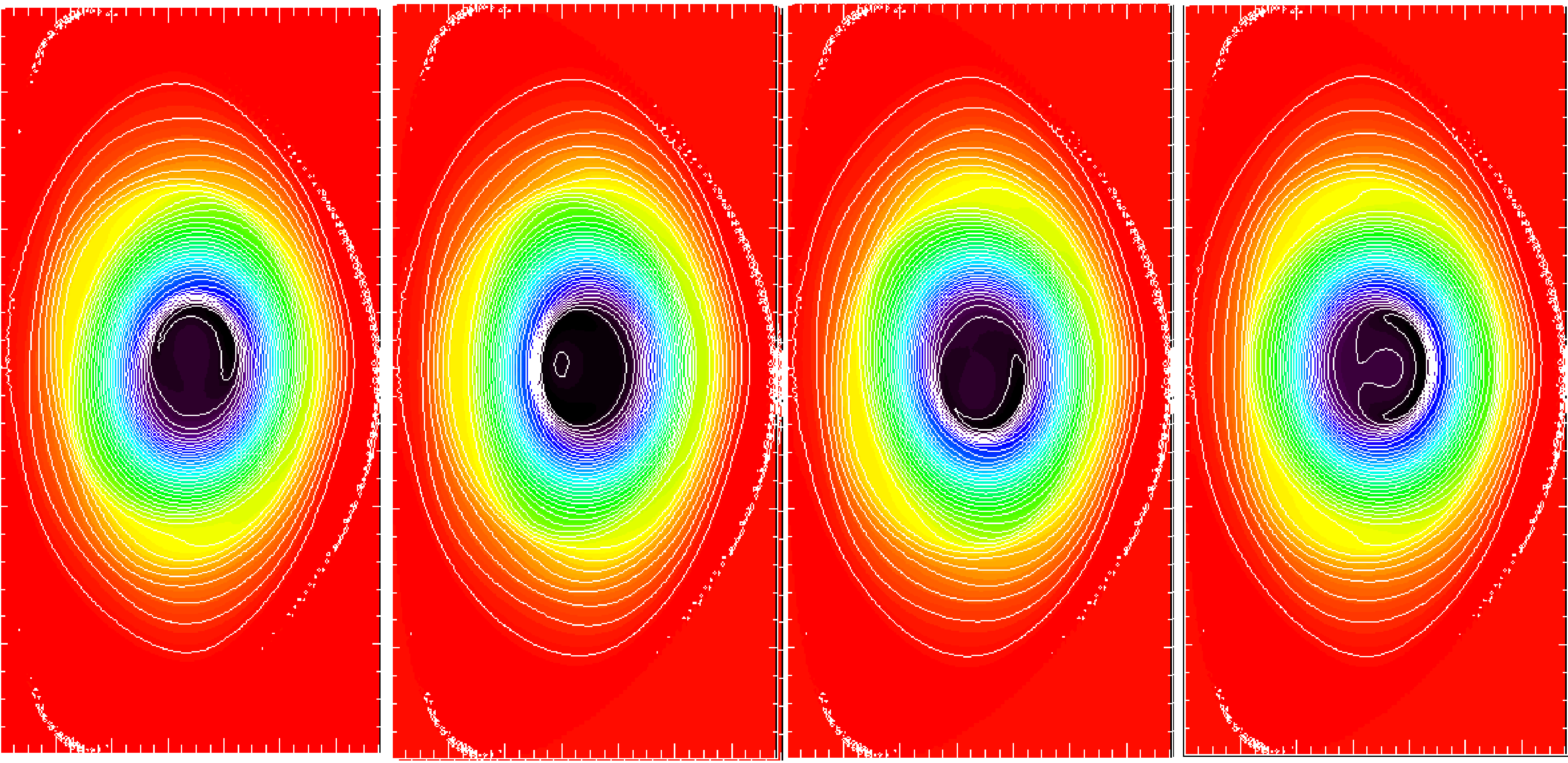

$\varphi = 0^o$ $\varphi = 90^o$ $\varphi = 180^o$ $\varphi = 270^o$

Stationary velocity stream function for DIII-D Oval (shot 118164)

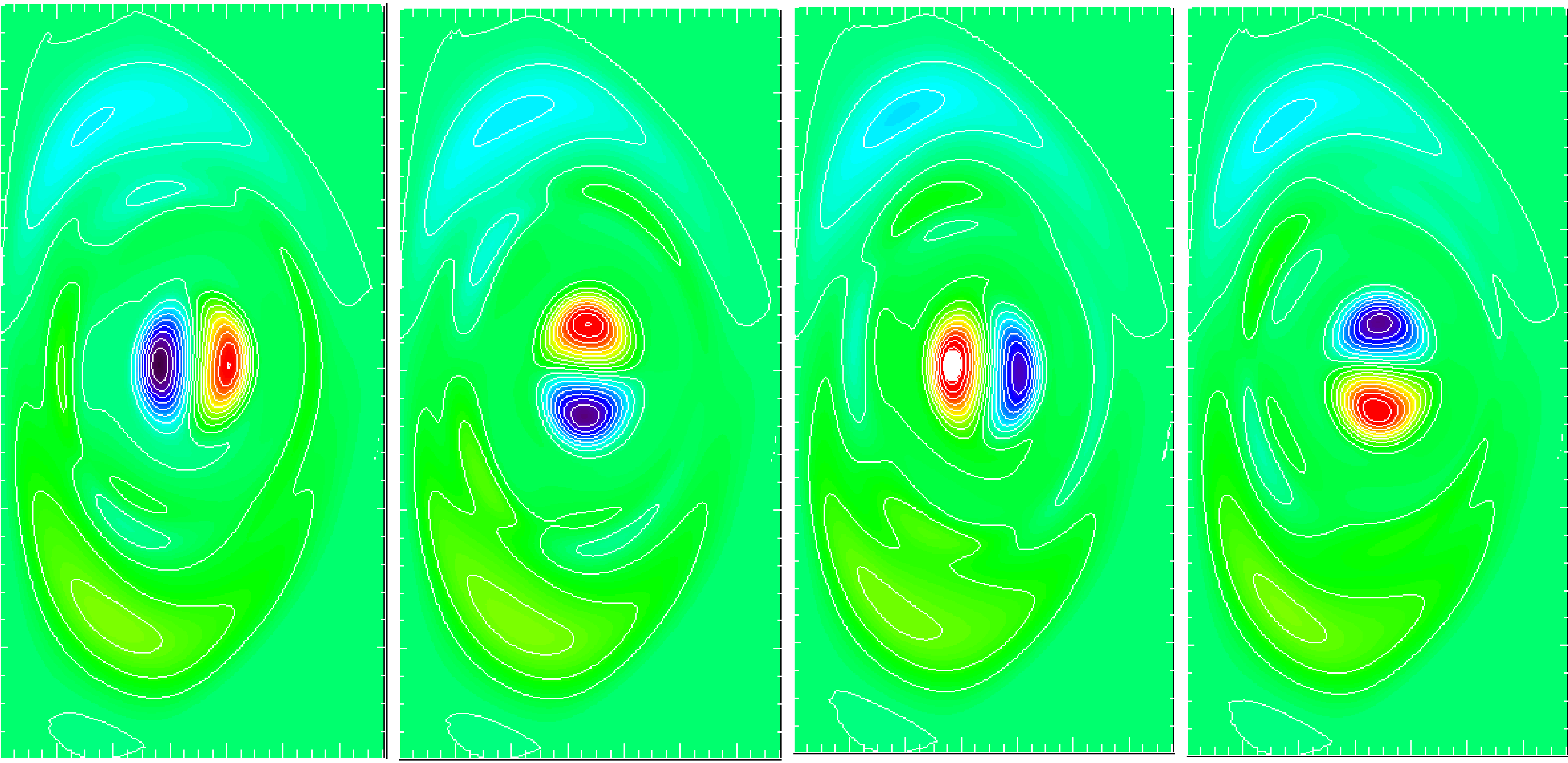

$\varphi = 0^o$ $\varphi = 90^o$ $\varphi = 180^o$ $\varphi = 270^o$

Oval stationary state has many islands

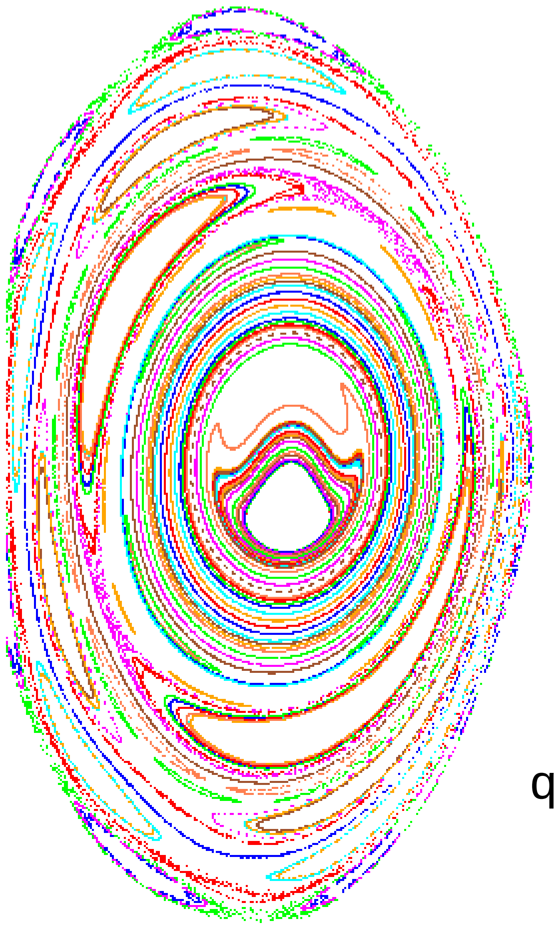

q_{min} = 1.01

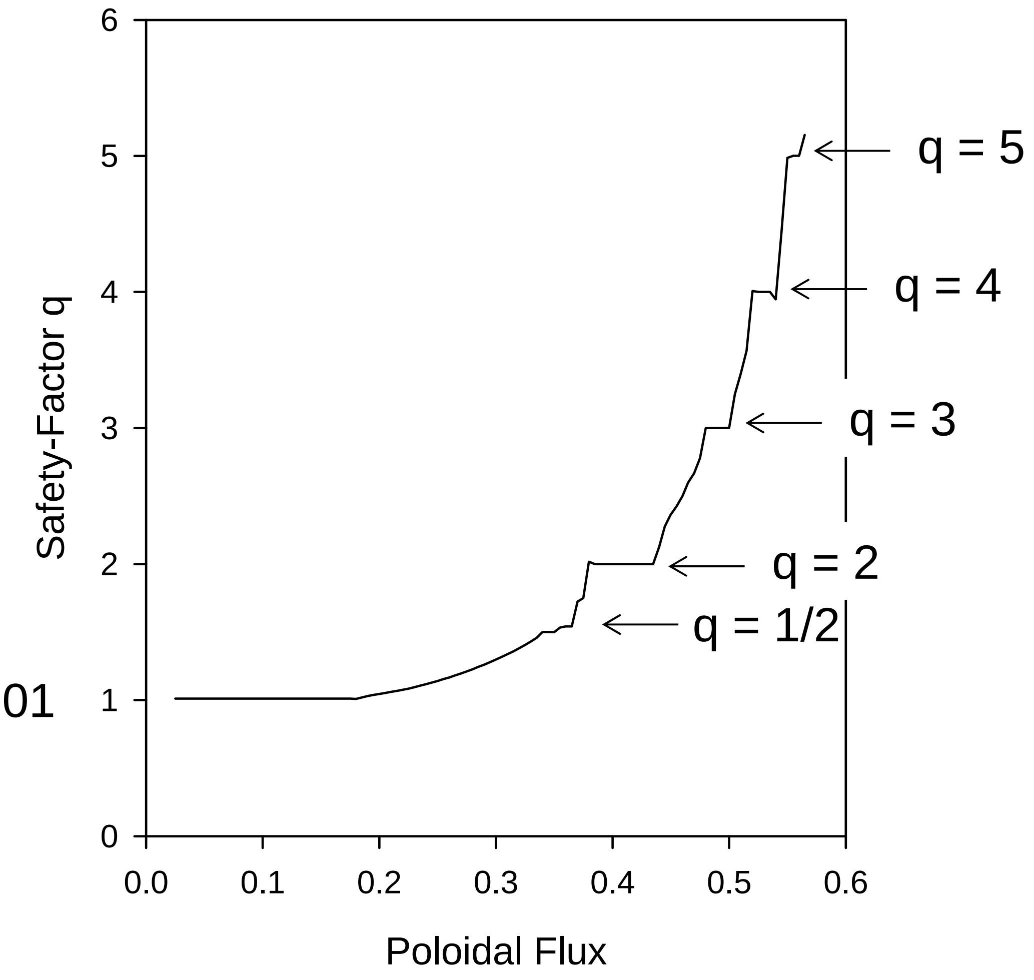

Summary

- 3D MHD in a highly magnetized high temperature plasma
  - Multiple timescales (ideal, reconnection, transport) demand implicit time advance
  - Implicit matrix contains large range of eigenvalues associated with the 3 different MHD wave types
- 3-step physics based preconditioner employed
  - Split implicit method reduces matrix size by 2 and makes matrix near symmetric and diagonally dominant
  - Annihilation operators approximately split matrix into 3 diagonal blocks, each with a greatly reduced condition number
  - Block Jacobi preconditioner dramatically reduces the condition number of each of the diagonal blocks
  - Final preconditioned matrix given to GMRES converges in 10s of iterations for fine zoned problem
- Recent Results
  - Repeating sawtooth demonstrate multiple timescale calculations
  - Stationary helical state can exist for some transport parameters

Extra Viewgraphs

In low viscosity runs, the periodic sawtooth dies out and a helical steady state is formed

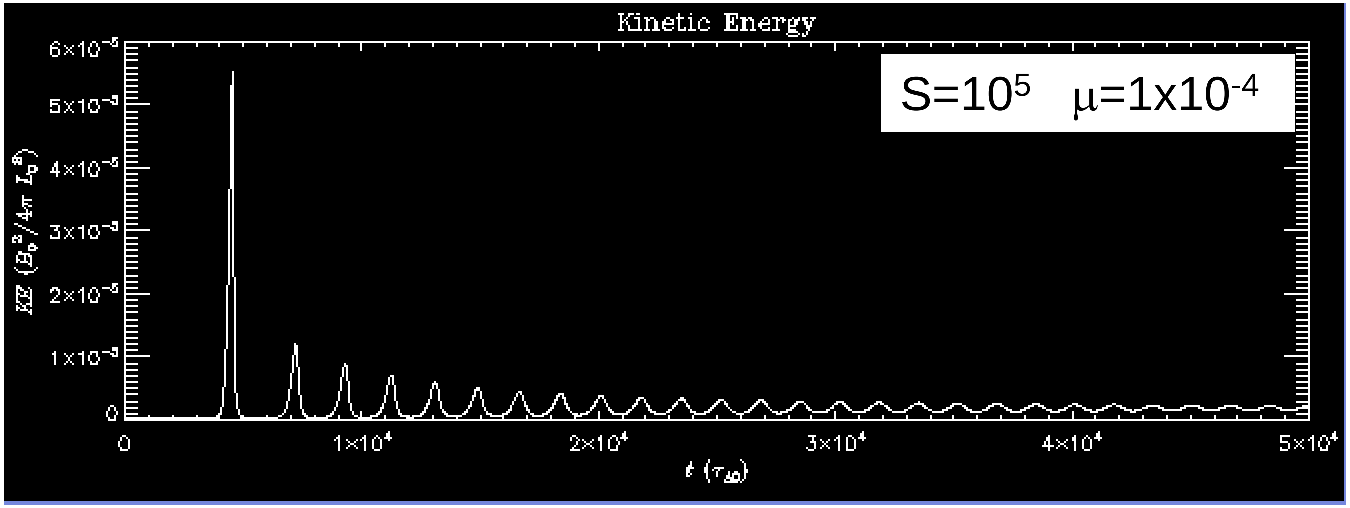

In higher viscosity runs, the periodic sawtooth remains

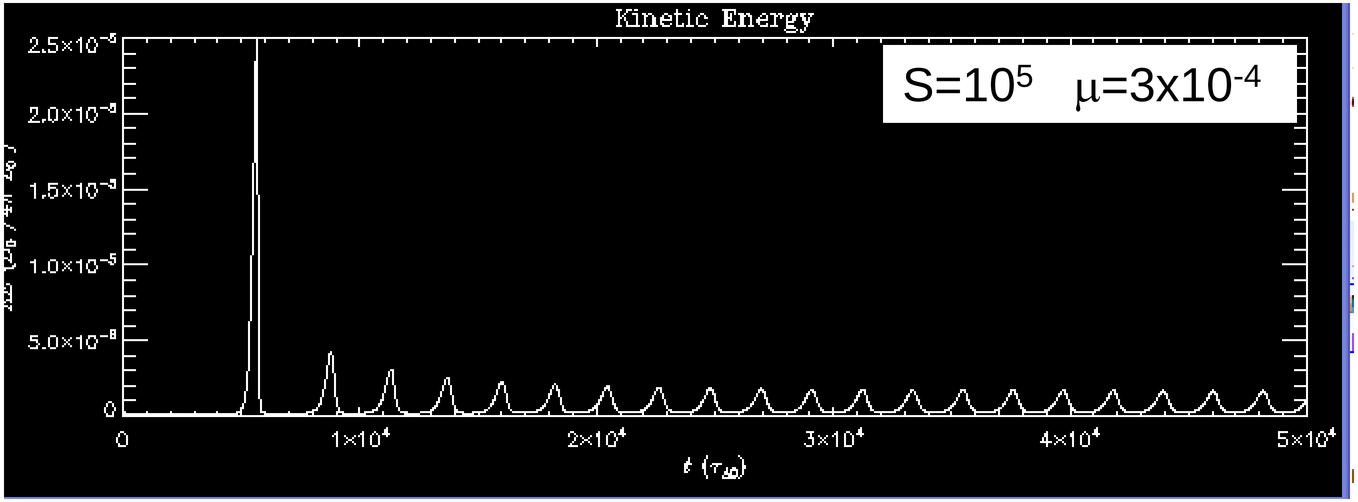

Low viscosity run settles down to stationary state where KE is constant in time

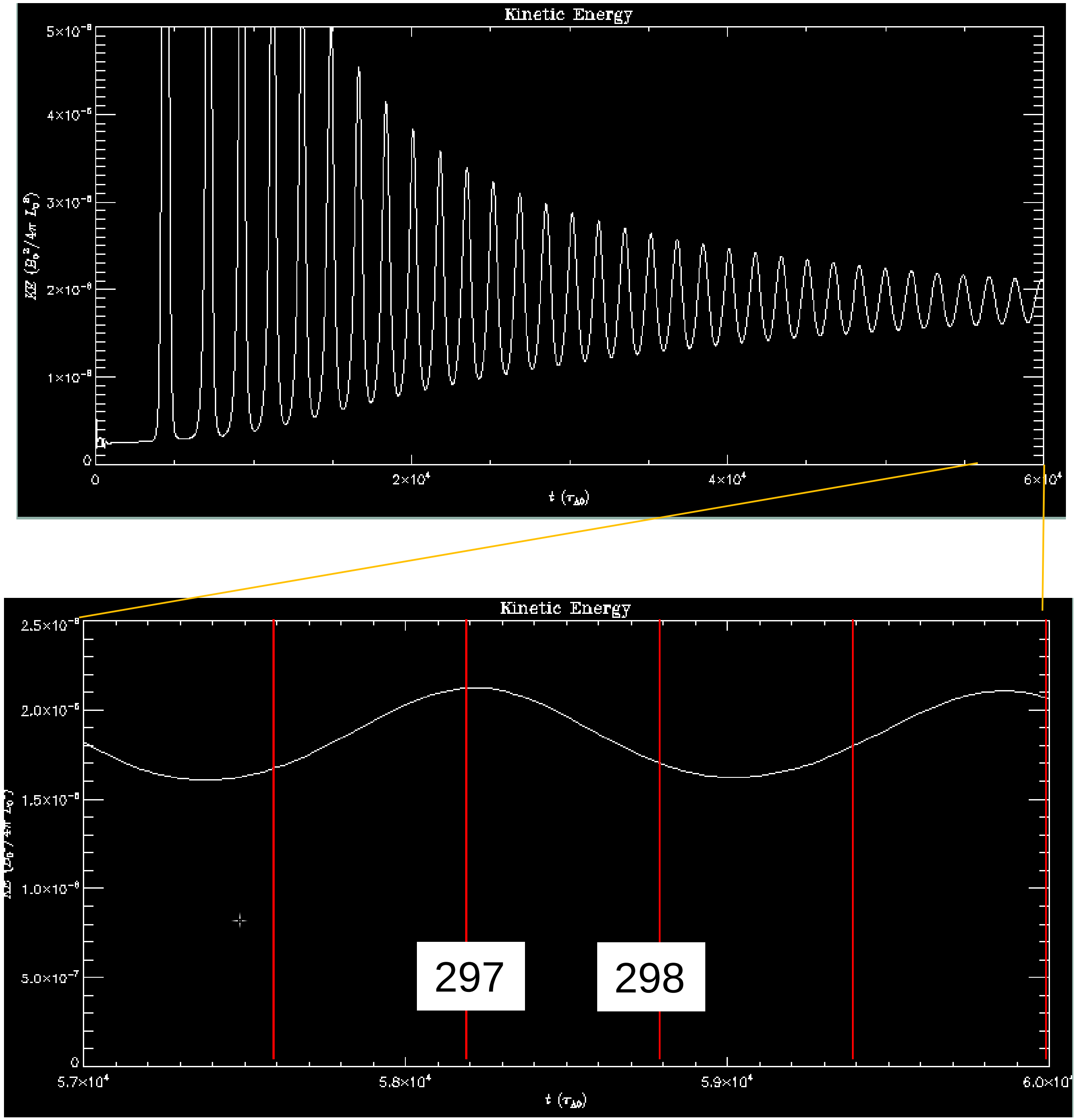

Poincare plots are very similar at peak and valley of kinetic energy.
Two magnetic axes.   Large region in center where q ~ 1

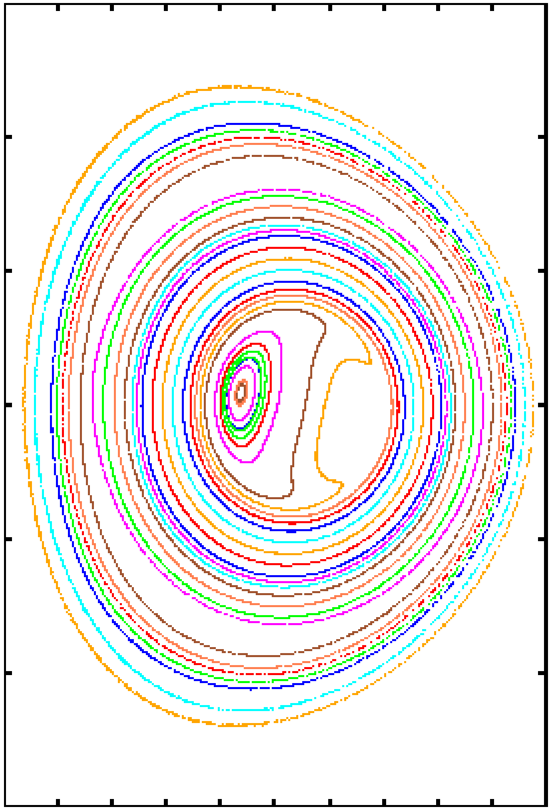

297

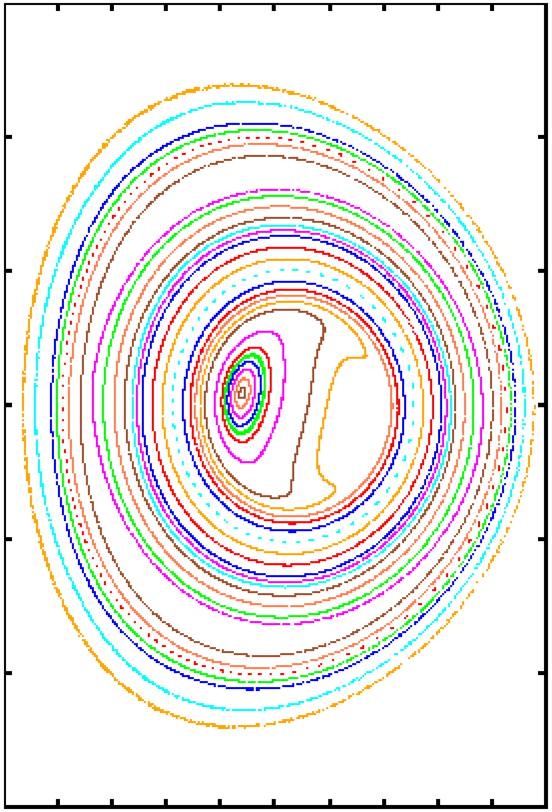

298

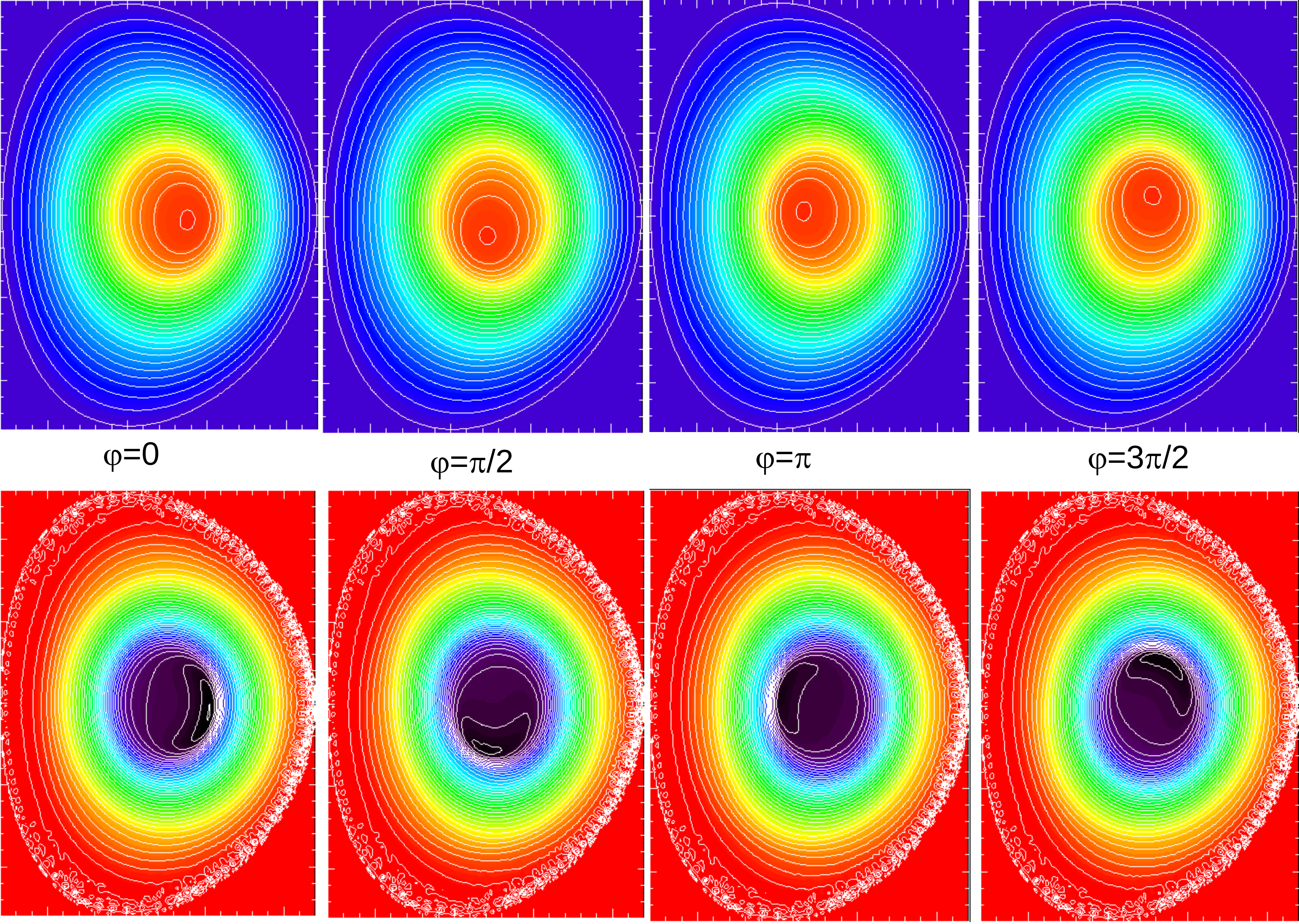

Helical distortion in central pressure (top) and toroidal current density

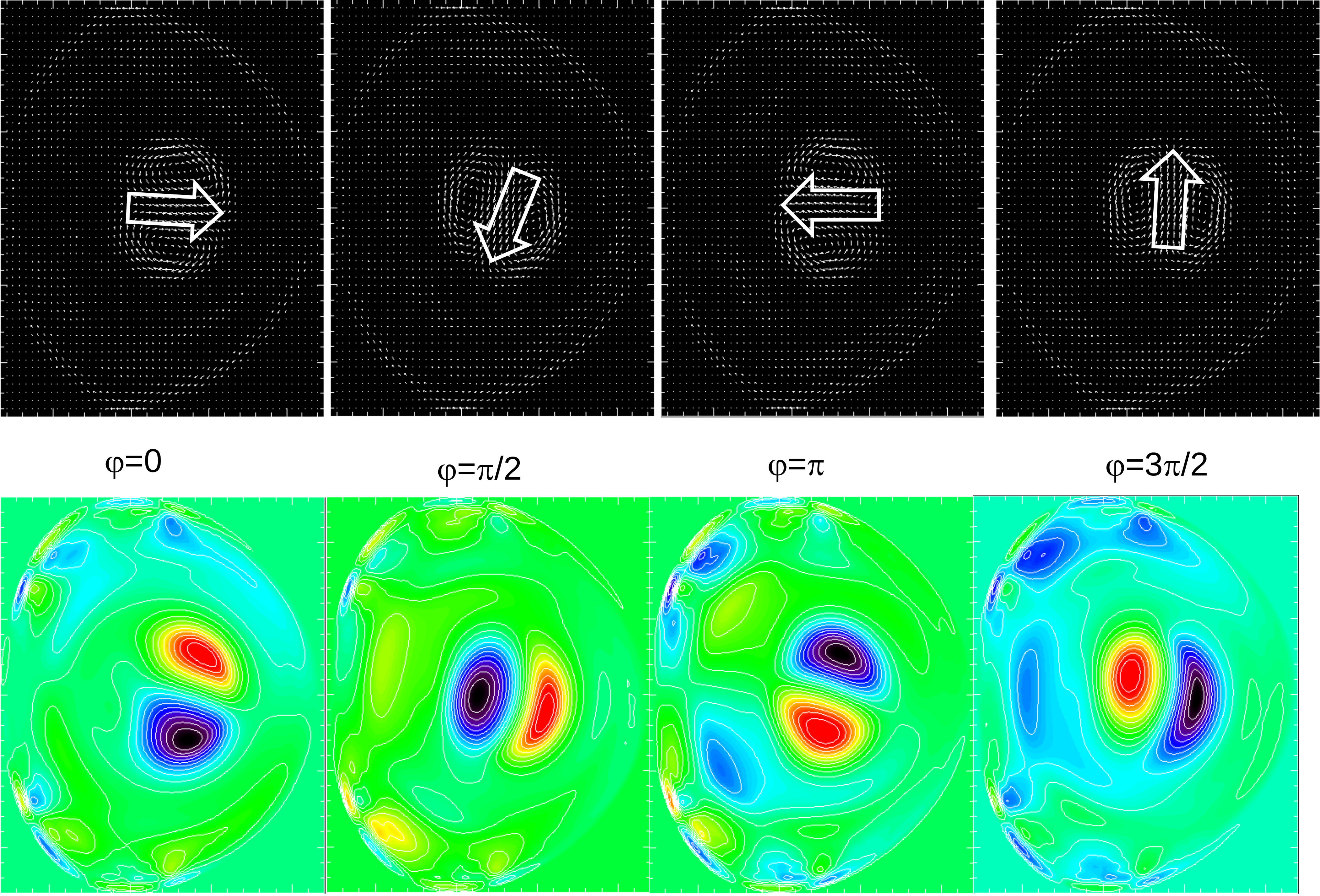

Poloidal velocity (top) and toroidal velocity(bottom) form stationary helical structures

Comparison of sawtooth cycles for $S=10^5$ and $S=10^6$

η/μ constant

Period:
~ $2000\tau_A$

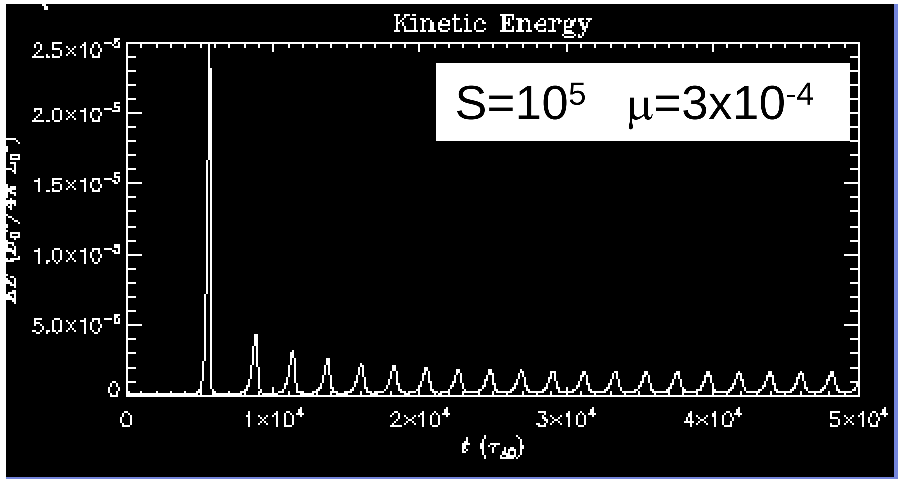

Period:
~ $9000\tau_A$

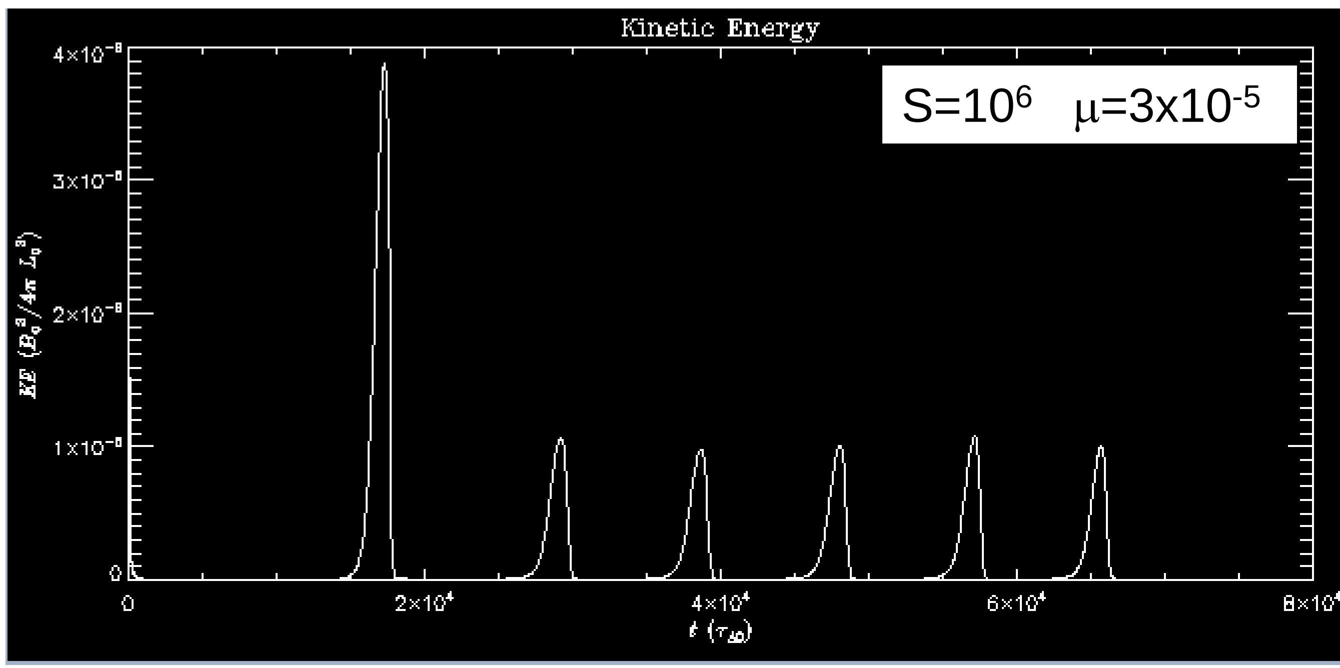

Form of the Vector Fields

(R,ϕ,Z)

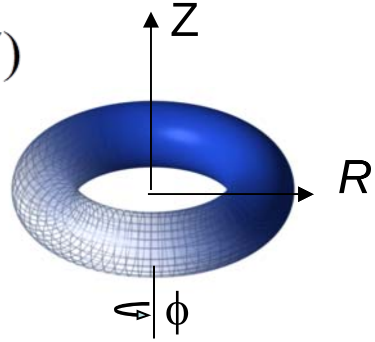

We express magnetic field in terms of two scalar fields such that $\nabla \bullet \mathbf{B} \equiv 0$ and it reduces to the standard form in 2D

$$\mathbf{A} = R^2 \nabla \phi \times \nabla f + \psi \nabla \phi - F_0 \ln R \hat{Z}$$

$$\mathbf{B} = \nabla \psi \times \nabla \phi - \nabla_\perp \frac{\partial f}{\partial \phi} + (F_0 + R^2 \nabla_\perp^2 f) \nabla \phi$$

$$= \nabla \psi \times \nabla \phi - \nabla \frac{\partial f}{\partial \phi} + (F_0 + R^2 \nabla^2 f) \nabla \phi$$

$$\mathbf{J} = \nabla (R^2 \nabla^2 f) \times \nabla \phi + \frac{1}{R^2} \nabla_\perp \frac{\partial \psi}{\partial \phi} - \Delta^* \psi \nabla \phi$$

Field from TF coils:

$$F_0 = \frac{\mu_0 I_{TF}}{2\pi}$$

Gauge condition:

$$R^2 \nabla_\perp \bullet \frac{1}{R^2} \mathbf{A} = 0$$

$$\nabla_\perp \equiv \nabla - \nabla \phi \frac{\partial}{\partial \phi}$$

In a standard tokamak, these satisfy the orderings:

$$f \ll \psi \ll F_0$$

This ordering is used, not to neglect terms, but to devise efficient and accurate numerical methods.

Momentum Equation Projections

Recall the form of the momentum equation we are using:

$$\text{(ME)} \quad \left\{\mathbf{I} - \theta^2 (\delta t)^2 L\right\} \mathbf{V}^{n+1} = \left\{\mathbf{I} - \theta^2 (\delta t)^2 L\right\} \mathbf{V}^{n} + \frac{\delta t}{\rho}\left\{-\nabla p + \frac{1}{\mu_0}(\nabla \times \mathbf{B}) \times \mathbf{B}\right\}^{n+1/2} + \cdots$$

To apply the Galerkin method we take the following annihilation projections, multiply by ν_i ,the i^{th} finite element basis function, and integrate over the domain

$$\iint d^3\tau\, \nu_i \nabla\varphi \bullet \nabla_\perp \times R^2 (\text{ME}) \quad \rightarrow \quad \iint d^3\tau\, R^2 \nabla_\perp \nu_i \times \nabla\varphi \bullet (\text{ME})$$

$$\iint d^3\tau\, \nu_i R^2 \nabla\varphi \bullet (\text{ME}) \quad \rightarrow \quad \iint d^3\tau\, \nu_i R^2 \nabla\varphi \bullet (\text{ME})$$

$$-\iint d^3\tau\, \nu_i \nabla_\perp \bullet R^{-2} (\text{ME}) \quad \rightarrow \quad \iint d^3\tau\, R^{-2} \nabla_\perp \nu_i \bullet (\text{ME})$$

Comparing expressions on right with the velocity field, we see that this is equivalent to multiplying by each term in the velocity.

$$\mathbf{V} = R^2 \nabla U \times \nabla\phi + R^2 \omega \nabla\phi + \frac{1}{R^2}\nabla_\perp \chi \qquad \int \mathbf{V} \bullet L = \delta W$$

Leads to (1) Discrete energy conserving equations, (2) Two energy conserving subsets (reduced MHD). Also, orthogonality property leads to (3) Separation of incompressible physics and (4) Well conditioned, diagonally dominant matrices.